ISSN: 4461 - 4780
Volume 15, Number 2, 2025
International Journal of Applied Science and Engineering

INVESTIGATION OF THERMAL EXPOSURE AND ITS INFLUENCE ON THE MECHANICAL BEHAVIOR OF HIGH-STRENGTH LOW-ALLOY (HSLA) STEELS"

[1]Emordi Ngozi Grace & [2]Ofili Joy Nkechi
[1,2]Department of Metallurgical Engineering, Delta State polytechnic Ogwashi-Uku, Nigeria,

ABSTRACT

This study investigates the effect of thermal exposure on the mechanical properties of 0.17% carbon High Strength Low Alloy (HSLA) steel, with annealing using Carbon Equivalent (CE) value. Steel samples were thermally subjected at temperatures ranging from 840°C to 990°C in 30°C increments, with soaking times of 30, 60, 90, and 120 minutes. samples were machine and evaluated for fatigue performance alongside other mechanical tests. Microstructural analysis was conducted using quantitative metallography with the point count method, while fractured surfaces were examined via scanning electron microscopy (SEM). Statistical analysis was performed using ANOVA and optimization techniques. The results reveal that increasing annealing temperature significantly enhances fatigue life, with samples annealed at 990°C exhibiting the highest fatigue cycles: 3.9×10^3 cycles at 321.31 MPa and 1.3×10^3 cycles at 1606.57 MPa. Samples annealed at 960°C showed comparable performance, while the control samples demonstrated the lowest fatigue resistance. Fatigue behavior, modeled using Basquin's equation, indicated that fatigue life is primarily influenced by the fatigue strength exponent (b), which decreases with increasing annealing temperature. In terms of hardness and impact properties, the sample annealed at 840°C recorded the highest hardness (129.4 BHN) but the lowest absorbed impact energy (58.75 J). Conversely, annealing at 990°C resulted in the lowest hardness (118.6 BHN) and the highest impact energy absorption (66.65 J). ANOVA confirmed the statistical significance of the variations in mechanical properties across the annealing conditions at a 95% confidence level. Consequently, this work demonstrates that controlled annealing significantly enhances the fatigue and impact performance of HSLA steel by optimizing its microstructure, thereby enhancing its suitability for demanding engineering and construction applications.

Key Words: Annealing, High Strength Low Alloy (HSLA) Steels

INTRODUCTION

Most engineering properties of metals and alloys are related to their atomic structure, crystal structure and microstructure. Mechanical properties are structure sensitive in nature and their magnitude depends largely on size, shape and distribution of various micro constituents. The mechanical properties of metals and its alloy can be changed by varying the relative proportions of micro constituents. This change in the mechanical properties can be achieved by exposure to thermal modifications. This is a process that constitute of heating a metal or alloy to a specific predetermined temperature, holding at this temperature for a required time and finally cooling from this temperature. All of these take place in the solid state.

Heat treatment originated as an ancient art in man's attempt to improve material performances in practical applications. It has a capability to considerably extend the service performance of materials. Metals and alloys develop requisite properties by heat treatment which plays a critical roles in achieving appropriate microstructure that imparts the desired characteristics in a given material. The goal is to achieve the desired microstructure in order to attain specific and defined properties which may be in its mechanical, physical, electrical or magnetic. Heat treatment changes the microstructures of metals, affecting mechanical properties like strength, ductility, resilience, hardness, and fatigue (Sreeteja ,2017). Annealing causes atoms tendency to move in the crystalline structure, as well as the number of dislocation motion decrease, resulting in

ductility and hardness changes. Annealing improves ductility, removes residual stresses caused by cold working or machine, and improves machinability. (Wang *et al.*, 1997).

High strength low alloy (HSLA) steels is a type of alloy steels that offer improved mechanical properties such as high strength and yield strength making them suitable for application requiring load bearing capability (Emordi et al, 2018). They have the ability of withstanding impact and deformation without fracture. This has endeared to the automotive industry for making different components including chassis, frames, and body panels where weight and light weight are needed. They also find wide application in the construction industry for the construction of bridges, and other infrastructural projects where strength and durability are needed. The oil and gas industry is not left out as it is used in production of pipe lines, and other equipment due to their strength and resistance to corrosion (ASM international 2001). It makes an impact to the preference for rigidity and weight loss in the Auto parts manufacturing. That's due to its excellent attributes of ability to be formed. Such steel alloys are useful in the manufacture of vehicle suspension mechanisms, support elements, horizontal beams, bending parts, and chassis are examples of such sections. (Kadkhodpour *et al*. 2011).

Lots of researchers have investigated on the heat treatments' effects and soaking times on the Steel characteristics (Zhuang, 2015; Offor et al., 2010; Kerscher et al., 2010; Sherman, 2016; Roselita, 2014; Senthil, 2016; Gaurav et al., 2018; Somer, 2007). Most of these researches conducted so far both on high strength low alloy, Plain Carbon and Stainless Steel have paid little or no attention to annealing at higher temperature and increased soaking time as a way to positively affect the mechanical properties of high strength low alloy Steels. This paper investigates the effect of heat treatment (annealing) and its significance on the mechanical properties of high strength low alloy(HSLA) steels

Review of Related Literature

According to the findings of the linked literature study, various researchers have investigated the effect of annealing temperature/soaking time on steels, with the majority of these researchers focusing on stainless steels in order to determine their impact on mechanical behavior. To the best of my knowledge, no research has been conducted on the influence of annealing temperature and time on fatigue and some mechanical properties of 0.17 percent C of High Strength Low Alloy steels. Although significant research has been done on the effect of fatigue on steel, little is known about the HEAT TREATMENT (ANNEALING) AND ITS SIGNIFICANCE ON THE MECHANICAL PROPERTIES OF HIGH STRENGTH LOW ALLOY (HSLA) STEELS.

MATERIALS AND METHODS

Materials were locally sourced (20 mm diameter rod of 0.17 percent HSLA Steel) It was then subjected to preliminary machining to remove its ribs, after which they were cut to **desired** sample specification according to the American Society for Testing and Materials (ASTM), 1990, and wire brushed before carrying out the heat treatment is carried out at 840^{o}C-990^{o}C with the as received not being heat treated. Thereafter subjected to mechanical testing

Table 1: Indicates the chemical constituents of the steel under consideration.

Element	C	Si	S	P	Cr	Mo	Ni	Al
Weight (%)	0.1728	0.3016	0.0352	0.0334	0.2559	<0.0100	0.1218	<0.0100
Element	Cu	Ti	Nb	W	Co	B	Fe	
Weight (%)	0.2560	<0.0100	<0.0150	<0.0500	<0.200	0.0047	97.304	

The materials used for the work was a 20 mm diameter rod of 0.17 percent Carbon high After machining, the samples were grouped for the different predetermined temperature and then normalizing was firstly done so as to remove internal stress incurred during machining. Before the annealing was done the Carbon equivalent was calculated to tell the starting temperature from the Iron Carbon phase diagram.

$$CE = C + \frac{Cr+Mo+V}{5} + \frac{Mn+Si}{6} + \frac{Ni+Cu}{15} \quad (1)$$

From the chemical composition in Table 1 above we have Cr = 0.2559, Mo = 0.0100, V = 0.0100, Mn = 1.2089, Si = 0.3016, Ni = 0.1218, Cu = 0.2560 and C=0.17

Substituting these figures in equation 1 above, we have

$$CE = 0.17 + \frac{0.2559+0.0100+0.0100}{5} + \frac{1.2089+0.3016}{6} + \frac{0.1218+0.2560}{15}$$

CE = 0.17 + 0.05518 + 0.25175 + 0.02513 = 0.50206 hence CE is 0.5. Hence, from the Iron Carbon phase diagram, the ideal starting point for annealing is 840^{o}C. Following the ascertainment of the temperature for which the annealing operation was carried out, the samples were subjected to different annealing temperatures starting from 840^{o}C to 990^{o}C at 30^{o}C interval and then soaked for 30 minutes to allow the heat get to the core of the samples. Mechanical testing (hardness and impact) were carried out and thereafter, the micro-structural analysis was done.

Hardness Testing

To determine the hardness, the Brinell hardness test was used. The brinell hardness test was performed on cut samples using a Monsato Tensometer in accordance with ASTM/A29M-15 (model W). Prior to the exam, A 10 mm hardened steel ball indenter was placed in a suitable holder, and a 10 mm hardened steel ball indenter was placed in a suitable holder and pushed into a prepared surface of the specimen; the surface would have been ground to 600 microns. A load of 750 kg was applied to the specimen on the machine and allowed for 15 minutes. The diameter of the ball's impression was determined using a Brinell Microscope, and the resulting Brinell hardness number was calculated. The Brinell Hardness Number (BHN) was got and used to plot the graph shown in Figures.

Testing for Impact

All specimens were subjected to impact testing in accordance with ASTM/A29M-15. The section thickness of these test specimens was measured. The experiments were carried out on a Hounsfield Impact Testing Machine using the Izod Impact Testing process. From 28 to 75 mm in length, the sample was notched at a 45^{o} angle. The amount of impact energy consumed by the specimen was measured in Joules using the machine's calibrated scale. Impact testing for all the specimens was done based on ASTM/A29M-15. Section thickness was determined using these test specimens.

Fatigue Test

The fatigue test was performed using the Avery Dennison fatigue monitoring unit it was conducted in the material testing laboratory/workshop of Obafemi Awolowo University Ile-Ife Osun State Nigeria. All specimens were subjected to fatigue testing in accordance with ***ASTM standard*** E606/E606M-12 the sample is fractured to failure by the application of a known value of reversed stresses which could be equal or un-equal in magnitude in both directions (positive and negative). The aim here is to evaluate the actual load of the material in question before failure. The number of failure cycles was registered by the motor's revolution counter. When the specimen splits, cut out switches connected to the computer automatically stop the machine.

Determination of Test Loads and the Bending Angles

It is therefore necessary that the testing load and the bending angle be calculated. From the 7505 fatigue testing manual the formulae below is used;

Stress $\sigma = \frac{Mmax}{W}$ 3.10

Where

M is bending moment read from the machine in Kg/cm

W is the section modulus = $\frac{\pi d^3}{32}$ 3.11

Conversion of Kg/cm to Nm is done by multiplying by 9.81 and dividing by 100 that is for 70KgfCm we have $\frac{70\times9.81}{100}$ =6.867Nm

How to calculate bending stress of the fatigue specimen

M$= \frac{E\pi d^3}{32L}$ 3.12

$\sigma_{B=}\frac{5.192m}{d^3}$ 3.13

Where

$\sigma_{B=}$ Bending stress

M=Bending moment only along the axes of the specimen to be bent into an angle

L= specimen's full length

D= Specimen's diameter

E= young modulus of the specimen depending on the specimen (Steel or Aluminium)

For steel, E=70$\times 10^3$N/m

Calculation of bending moment for 840^o C at 120 minutes soaking time

M$= \frac{E\pi d^3}{32L}$

Where E =70x10^3 N/m

d= 5x 10^{-3}

L= 45.3 x10^{-3}

Substituting into Equation3.13 we have

M$= \frac{70x3.14x5^3}{32x45x10^{-3}}$

$\sigma_{B=}\frac{5.192m}{d^3}$ 3.13

For $\sigma_{B=}$ Bending stress we have

$\sigma_{B=}$ $\sigma_{B=}\frac{5.192m}{5^3x10^{-3}}$

3.0 Results and Discussions

Results of Annealing Temperatures on Impact and Hardness

The graphs below (Figure 1to Figure 4) present the hardness and impact results obtained from the annealed steel samples at different soaking times (30minutes, 60minutes, 90 minutes and 120minutes) with the control for comparison.

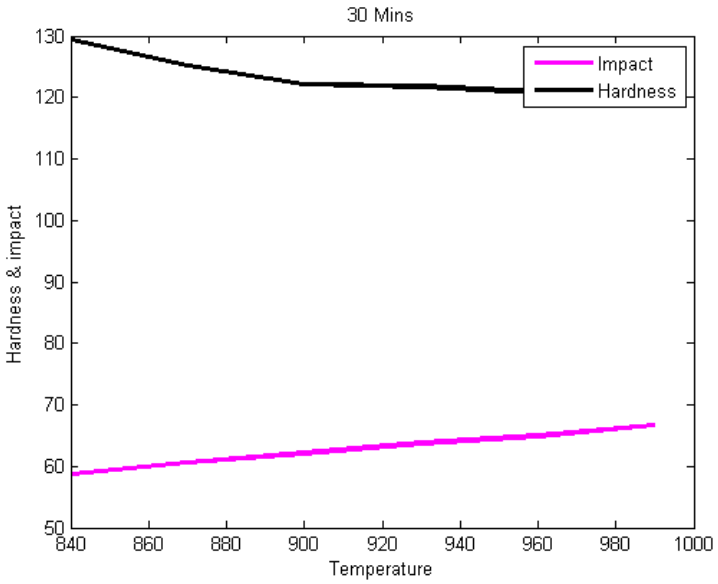

Figure 1 Effect of Annealing Temperatures on Hardness and Impact for 30 minutes Soaking Time

Figure 1 illustrates the influence of annealing temperature on impact and hardness after soaking for 30 minutes. The graph shows that as the temperature rises, the impact increases from 58.75J at 840°C to 66.65J at 990°C, while the hardness steadily decreases from 129.4(BHN) at 840°C to 118.6(BHN) at 990° C, the annealing temperature with the lowest hardness.

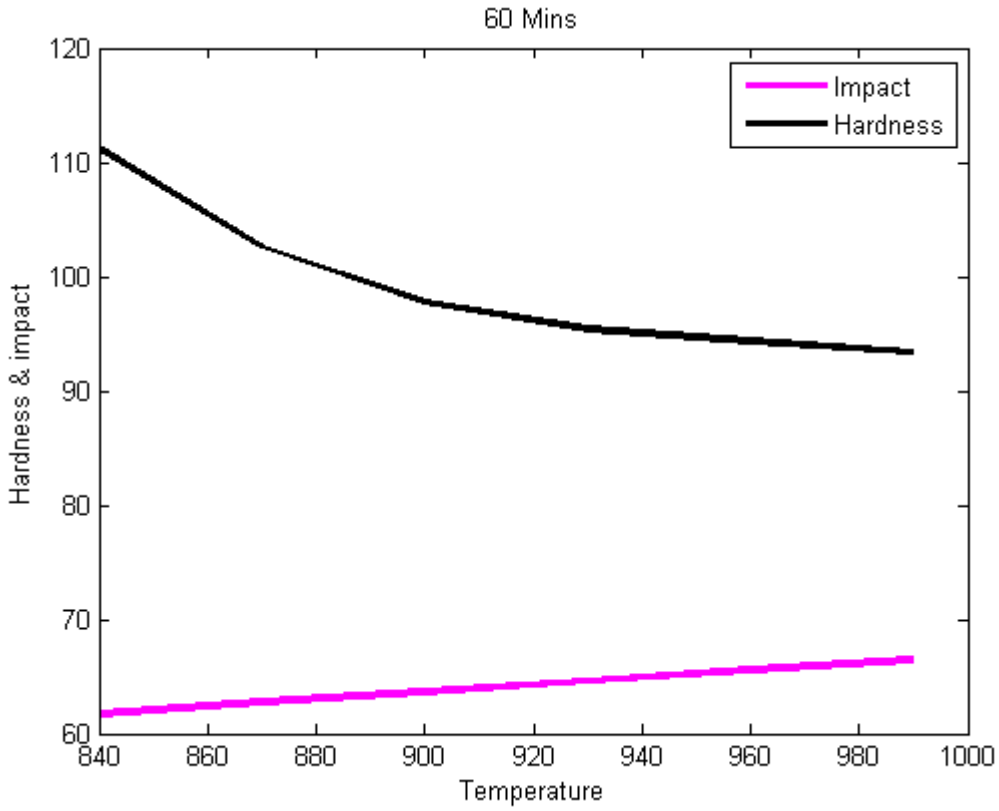

Figure 2 Effect of Annealing Temperatures on Hardness and Impact for 60 minutes Soaking Time

Figure 2 explains the result of annealing temperature on impact and hardness over a 60-minute soaking time; the graph shows that as the annealing temperature increases, the impact increases from 61.69 J at 840°C to 66.49 J at 990°C; the hardness peaks at 840 °C with 111.3 BHN and gradually decreases from 111.3(BHN) to 93.36(BHN) at 990°C where we saw the least hardness.

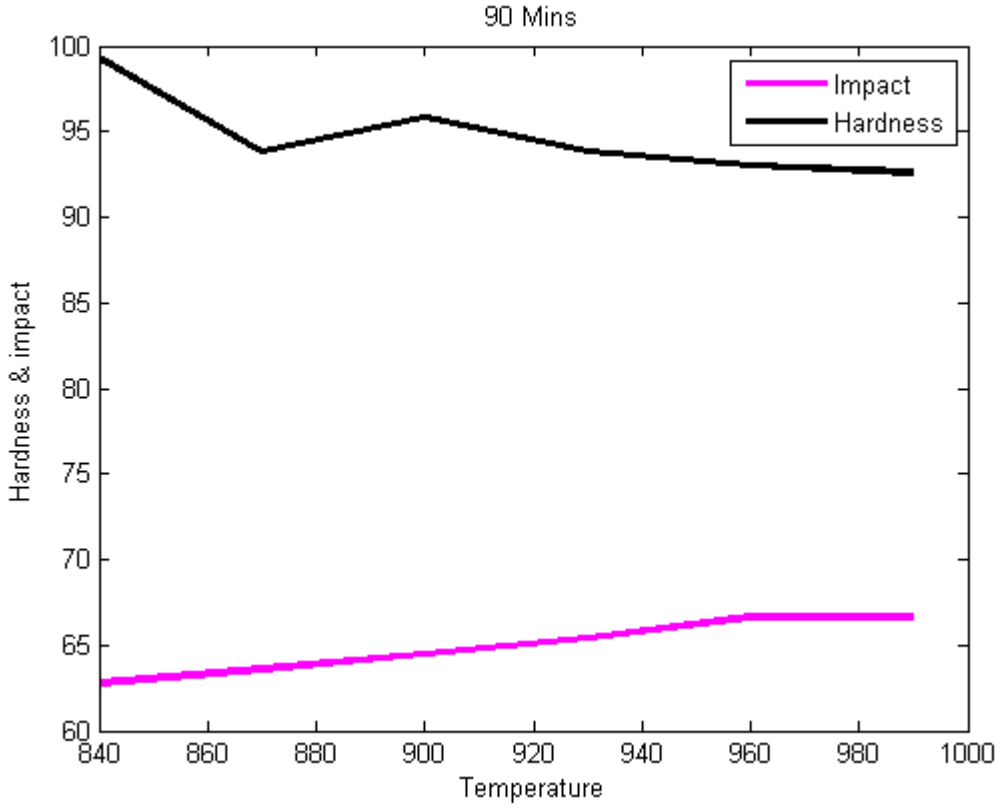

Figure 3 Effect of Annealing Temperatures on Hardness and Impact for 90 Minutes Soaking Time

Figure 3 depicts the impact and hardness effects of annealing temperature over a 90-minute soaking period. The graph shows that as the temperature rises, the impact increases from 62.79J at 840°C to 66.63J at 990°C, where the impact is highest, while the hardness steadily decreases from 99.8 (BHN) at 840°C to 92.6(BHN) at 990° C annealing temperature, where the hardness is lowest.

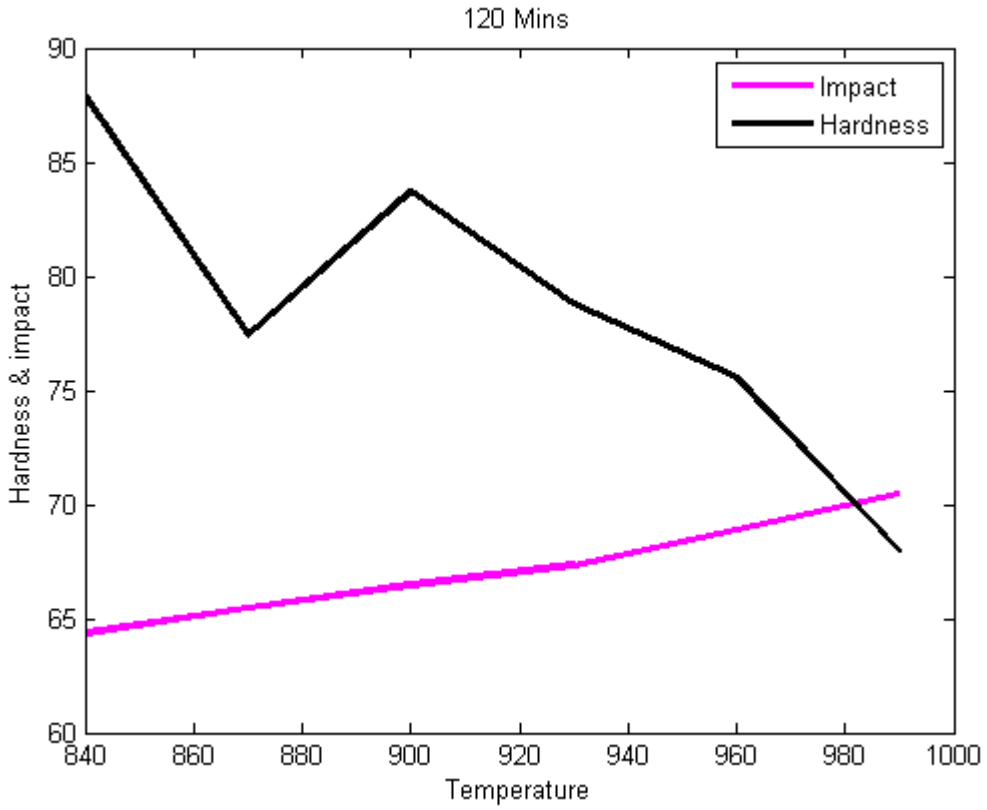

Figure 4 Effect of Annealing Temperatures on Hardness and Impact for 120 minutes Soaking Time

Figure 4 portrays the influence of annealing temperature on impact and hardness after soaking for 120 minutes. The graph shows that as the temperature rises, the impact increases from 64.37J at 840°C to 66.63J at 990°C, where the impact is highest, while the hardness steadily decreases from 99.8 (BHN) at 840°C to 92.6(BHN) at 990° C annealing temperature, where the hardness is lowest.

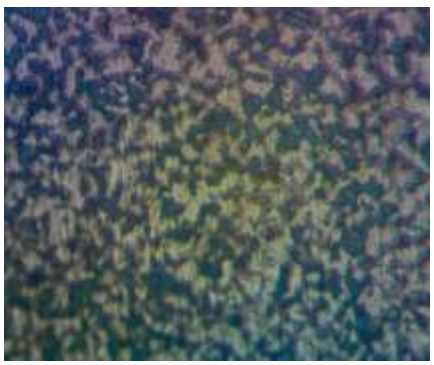

Plate 1 Microstructure of Specimen held at 840°C for 30 Minutes

Plate depicts the microstructure of a heat-treated (annealed) sample obtained after 30 minutes of keeping time at 840°C annealing temperature. The micrograph reveals uniform distribution of ferrite. From the point count calculations, the ratio percentage of ferrite to cementite is 44:56.

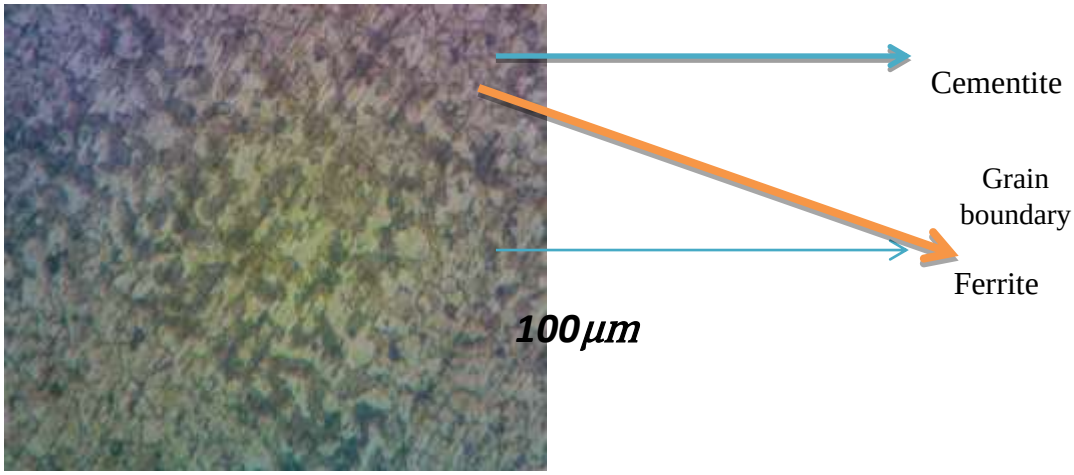

Plate 4.1b
Microstructure of Specimen held at 870^{0}C for 30 Minutes

Plate 4.1b displays the microstructure of a heat-treated (annealed) sample obtained at an annealing temperature of 870^{o}C and a holding time of 30 minutes. The micrograph shows that as the annealing temperature increases, cementite non- uniformly distributes in the microstructure of the heat treated specimen. The results obtained from the point count calculations; the percentage ferrite to cementite is 42: 58 %

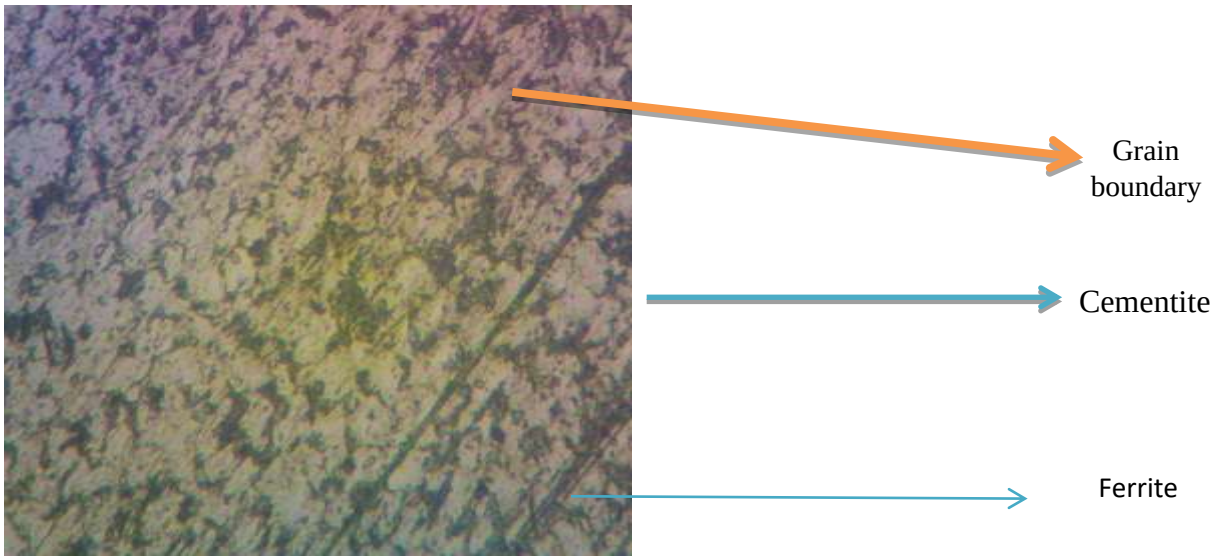

Plate 4.1c **Microstructure of Specimen held at 900^{0}C for 30 Minutes**

Plate 4.1c shows the result of the microstructure of the heat-treated (annealed) sample got at 900^{o}C annealing temperature and 30 minutes holding time. The micrograph shows that as the annealing temperature increases, ferrite and cementite are seen to be of almost equal proportion in the microstructure. The point count calculations gave a 50:50 percentage ratio of ferrite and cementite.

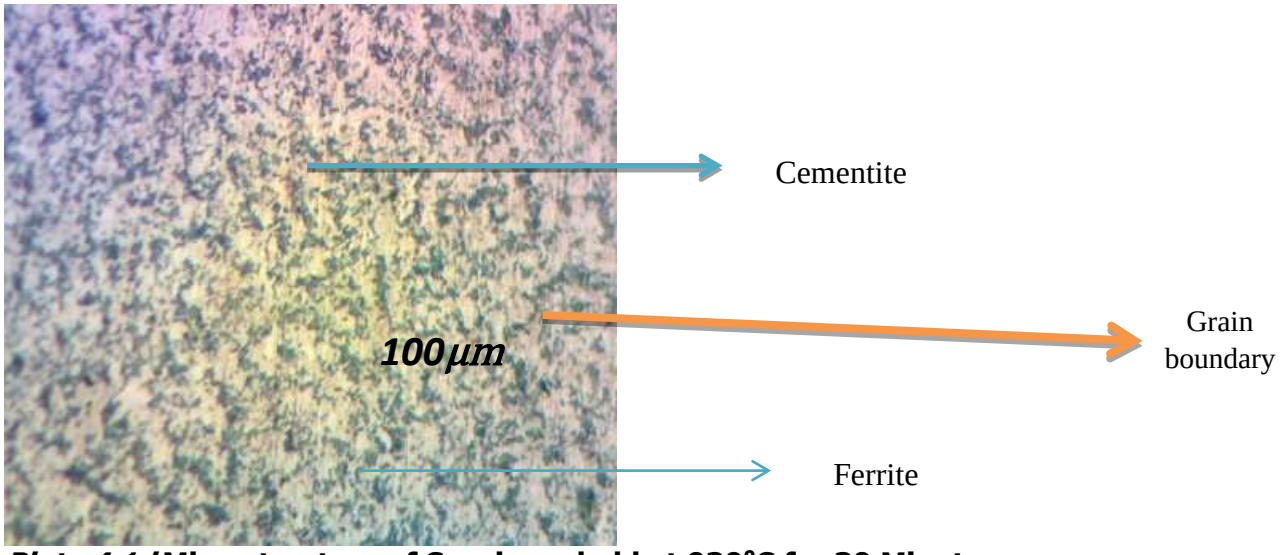

Plate 4.1d **Microstructure of Specimen held at 930^{0}C for 30 Minutes**

In Plate 4.1d, you can see the microstructure of the sample which was heat treated at 930^{o}C for 30 minutes. The micrograph shows that as the annealing temperature increases, cementite is seen to dominate while ferrite is randomly scattered in the microstructure. From the point count calculations; the percentage ratio of ferrite to cementite is 40: 60.

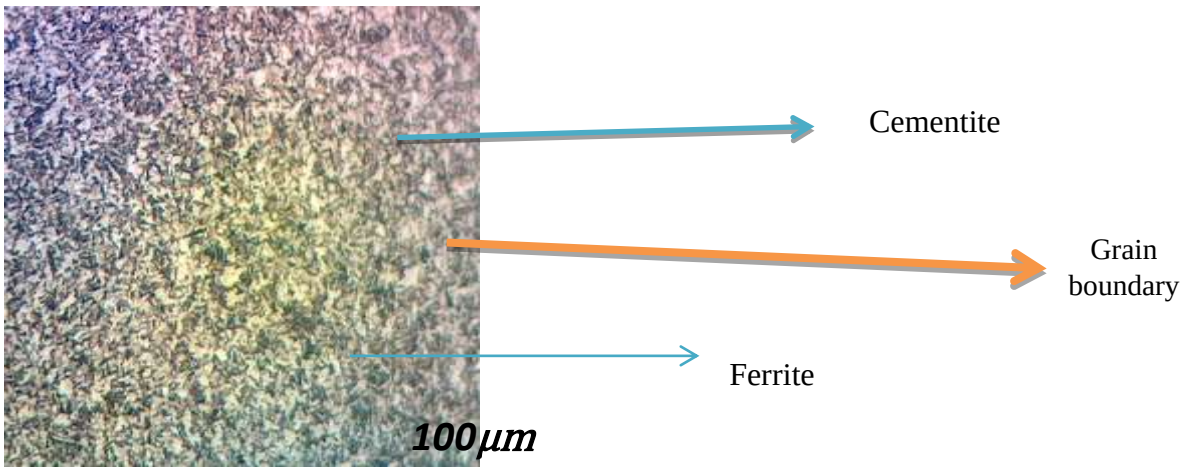

Plate 4.1e **Microstructure of Specimen held at 960^{0}C for 30 Minutes**

Plate 4.1e depicts the microstructure of a heat-treated (annealed) sample collected at an annealing temperature of 960^{o}C and a holding time of 30 minutes. The micrograph shows that as the annealing temperature rises, the grain size changes, cementite increases, and ferrite is randomly distributed in the microstructure. The grain boundaries, however, are not visible. According to the point count calculations, the percentage ratio of ferrite to cementite is 50:50.

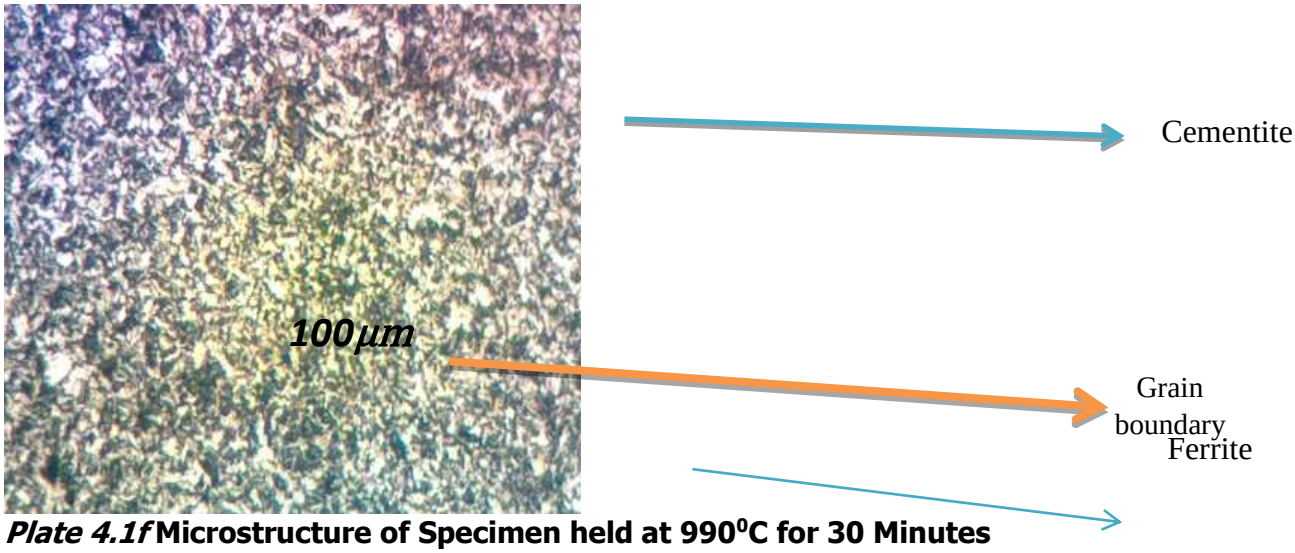

Plate 4.1f **Microstructure of Specimen held at 990^{0}C for 30 Minutes**

Plate 4.1f depicts the microstructure of a heat-treated (annealed) sample collected at an annealing temperature of 990^{o}C and a holding time of 30 minutes. The micrograph shows that as the annealing temperature increases, the grain size appears to be bigger than that of 960^{o}C cementite is seen to be more while ferrite is randomly scattered in the microstructure. However, the grain boundaries are not seen to be visible. Results from the point count calculation show a 47% of ferrite and 53% of cementite.

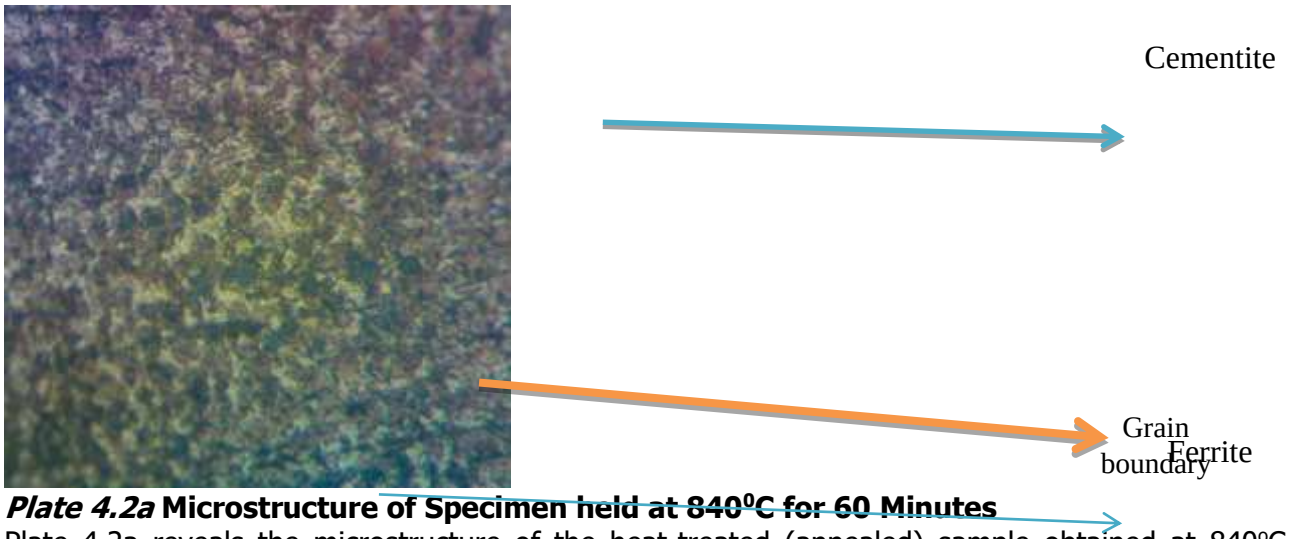

Plate 4.2a **Microstructure of Specimen held at 840^{0}C for 60 Minutes**

Plate 4.2a reveals the microstructure of the heat-treated (annealed) sample obtained at 840^{o}C annealing temperature at 60 minutes holding time. The micrograph shows, ferrite has been non-uniformly distributed in the microstructure with cementite dominating. It could also be observed that the grains are changed while the grain boundaries appear not visible. The point count calculation shows that the percentage of ferrite to cementite is 40: 60.

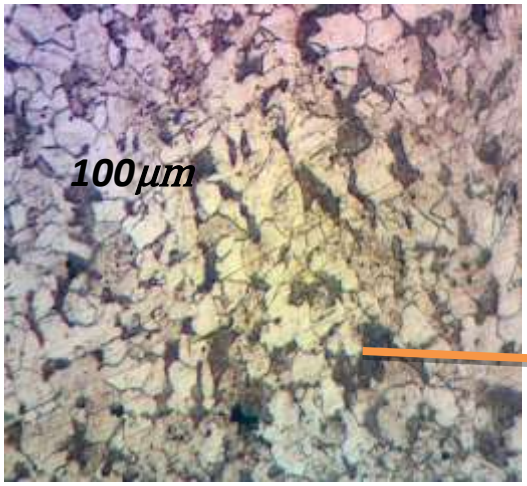

Plate 4.2b **Microstructure of Specimen held at 870^{0}C for 60 Minutes**

Plate 4.2b depicts the result of the microstructure of the heat-treated (annealed) sample got at 870^{o}C annealing temperature at 60 minutes holding time. The micrograph reveals that as the annealing temperature increases, cementite is seen to non- uniformly distributed in the microstructure with ferrite dominating. It could also be observed that the grains are changed while the grain boundaries appeared visible. The point count calculation gave 80:20 ratio of ferrite to cementite.

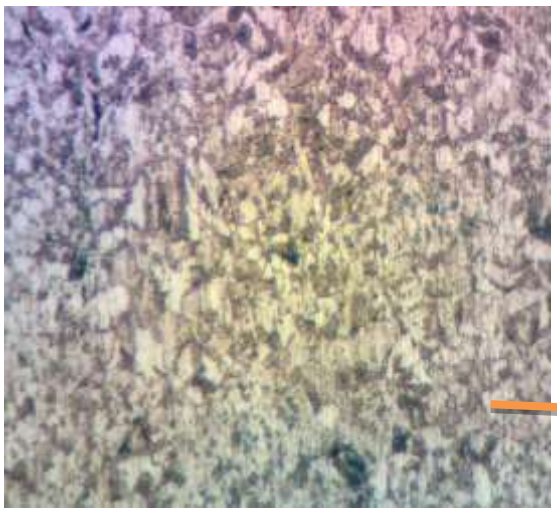

Plate 4.2c **Microstructure of Specimen held at 900^{0}C for 60 Minutes**

Plate 4.2c reveals the microstructure of a heat-treated (annealed) sample obtained at 900^{o}C annealing temperature and 60 minutes holding time. The micrograph shows that as the annealing temperature increases, ferrite is seen to be uniformly distributed in the microstructure and dominating while cementite is seen to be sparingly distributed in the microstructure. It could also be observed that the grains are changed while the grain boundaries appear not visible. From the point count calculations, the percentage of ferrite to cementite is 65:35.

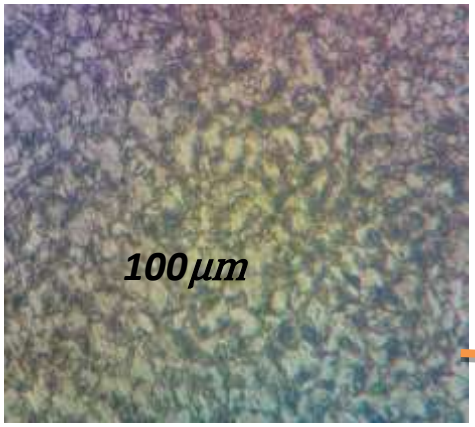

Plate 4.2d **Microstructure of Specimen held at 930^{0}C for 60 Minutes**

Plate 4.2d depicts the microstructure of a heat-treated (annealed) sample got at 930^{o}C annealing temperature and 60 minutes holding time. The micrograph shows that as the annealing temperature increases, ferrite is seen to be non- uniformly distributed in the microstructure while cementite is seen to have dominated. It could also be observed that the grains are changed while the grain boundaries appear not visible. The point count calculations show that the percentage of ferrite to cementite is 30: 70.

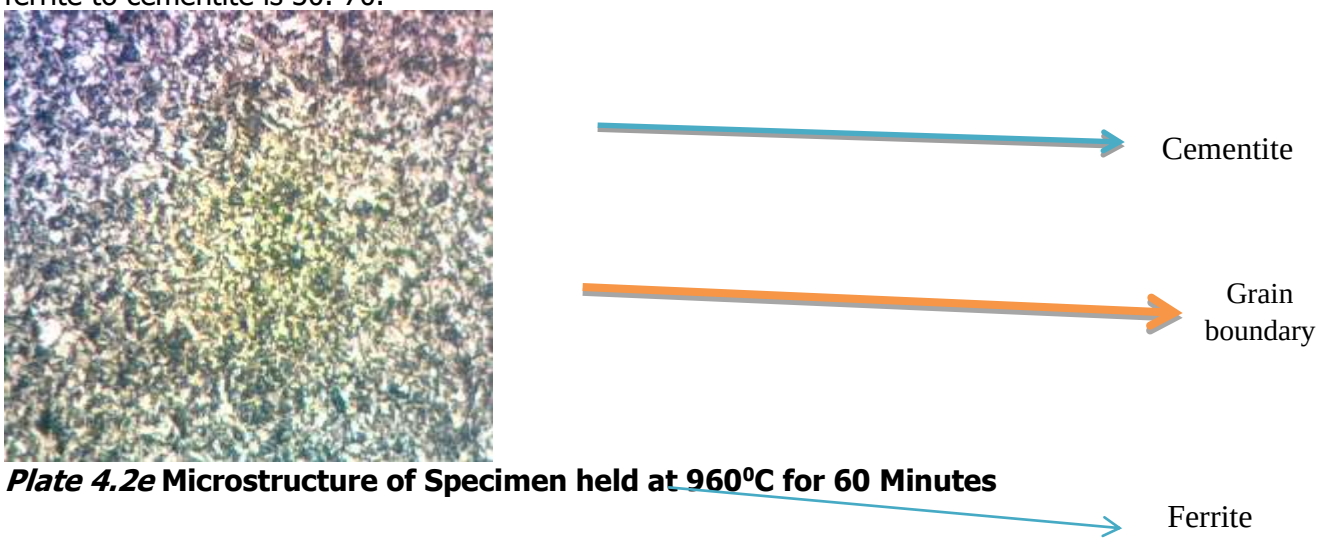

Plate 4.2e **Microstructure of Specimen held at 960^{0}C for 60 Minutes**

The microstructure of the heat-treated (annealed) sample obtained at 960^{o}C annealing temperature and 60 minutes holding time is shown in Plate 4.2e the micrograph reveals that as the annealing temperature increases, ferrite is seen to be uniformly distributed in the microstructure while cementite is seen to more in percentage. It could be observed also that the grains are changed while the grain boundaries appear not visible. The point count calculation results gave the percentage ratio of ferrite to cementite as 43:57.

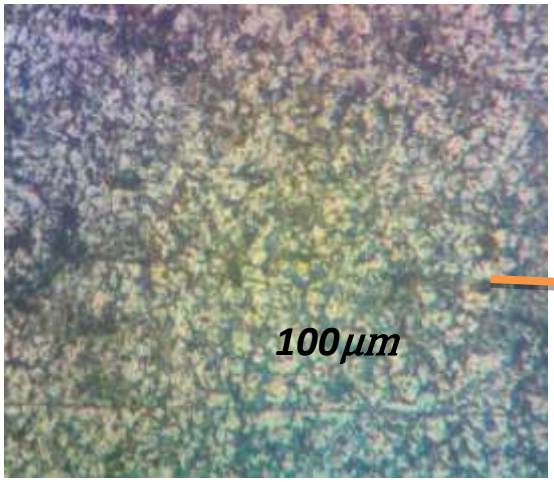

Plate 4.2f **Microstructure of Specimen held at 990^{0}C for 60 Minutes**

The microstructure of the heat-treated (annealed) sample obtained at 990^{o}C annealing temperature and 60 minutes holding time is shown in Plate 4.2f. The micrograph reveals that as the annealing temperature increases, ferrite is seen to be uniformly distributed in the microstructure while cementite is seen to more in percentage. It could be observed also that the grains are changed than those of 960^{o}C while the grain boundaries appear not visible. Results from the point count shows that the ratio of ferrite to cementite is 48:52.

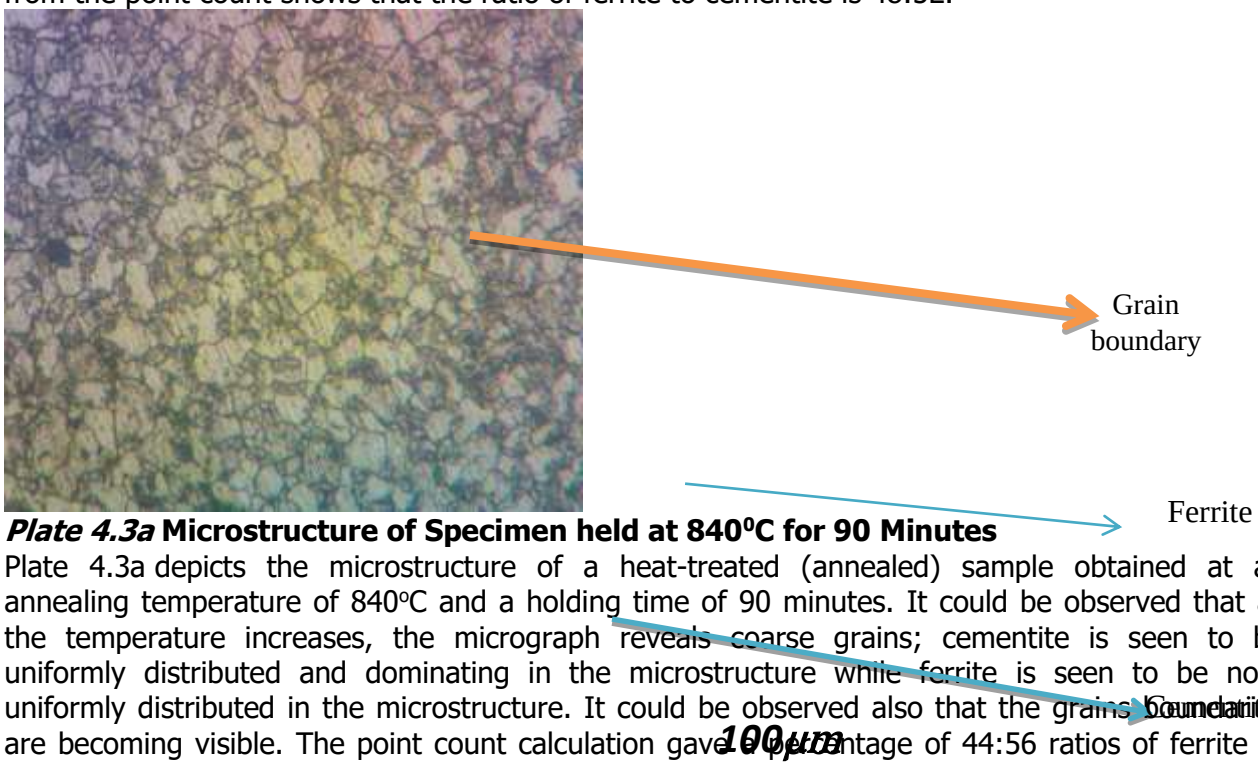

Plate 4.3a **Microstructure of Specimen held at 840^{0}C for 90 Minutes**

Plate 4.3a depicts the microstructure of a heat-treated (annealed) sample obtained at an annealing temperature of 840^{o}C and a holding time of 90 minutes. It could be observed that as the temperature increases, the micrograph reveals coarse grains; cementite is seen to be uniformly distributed and dominating in the microstructure while ferrite is seen to be non-uniformly distributed in the microstructure. It could be observed also that the grains boundaries are becoming visible. The point count calculation gave a percentage of 44:56 ratios of ferrite to Cementite.

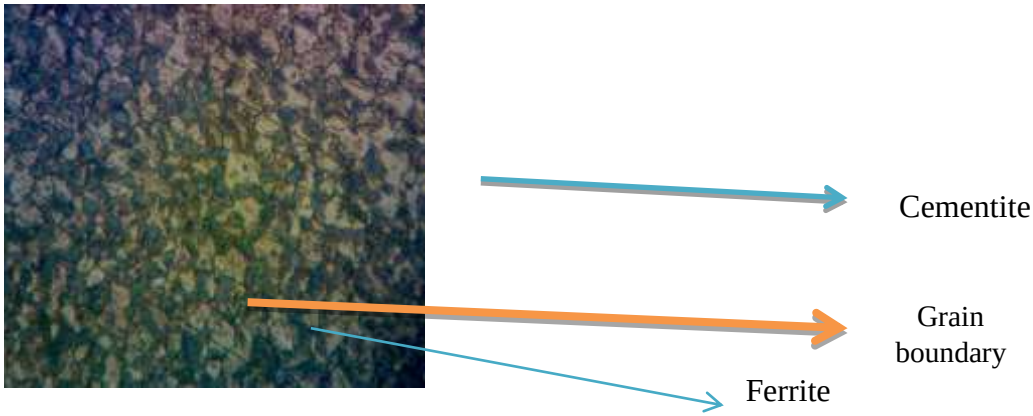

Plate 4.3b **Microstructure of Specimen held at 870^{0}C for 90 Minutes**

Plate 4.3b depicts the microstructure of a heat-treated (annealed) sample obtained at an annealing temperature of 870°C and a holding time of 90 minutes. As the temperature rises, the micrograph exposes coarse grains; cementite and ferrite are seen to be evenly dispersed in the microstructure, and grain boundaries are visible. The point count calculation revealed an equal number of ferrite to cementite ratio.

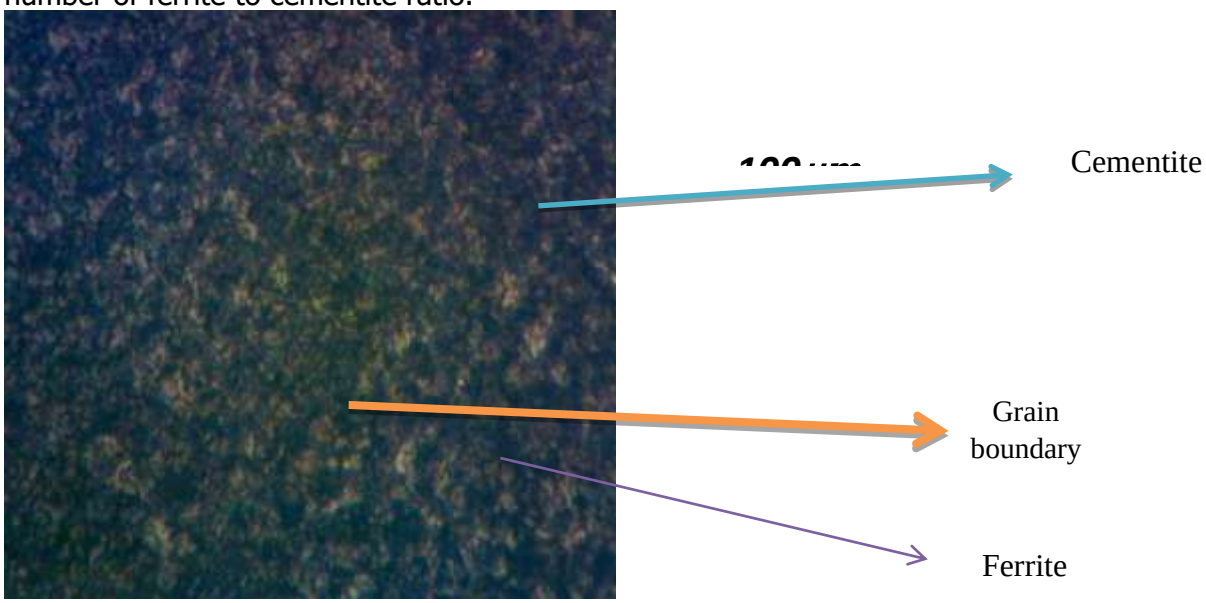

Plate 4.3c Microstructure of Specimen held at 900^{0}C for 90 Minutes

Plate 4.3c depicts the microstructure of a heat-treated (annealed) sample obtained at an annealing temperature of 900°C and a holding time of 90 minutes. It could be observed that as the temperature increases, the micrograph reveals less coarse grains hence more grain boundaries; cementite is seen to be uniformly distributed and dominating in the microstructure while ferrite is seen to be non-uniformly distributed in the microstructure. It could be observed also that the grains boundaries were invisible. Results from the point count shows that ferrite is 48% in the microstructure while cementite is 52%.

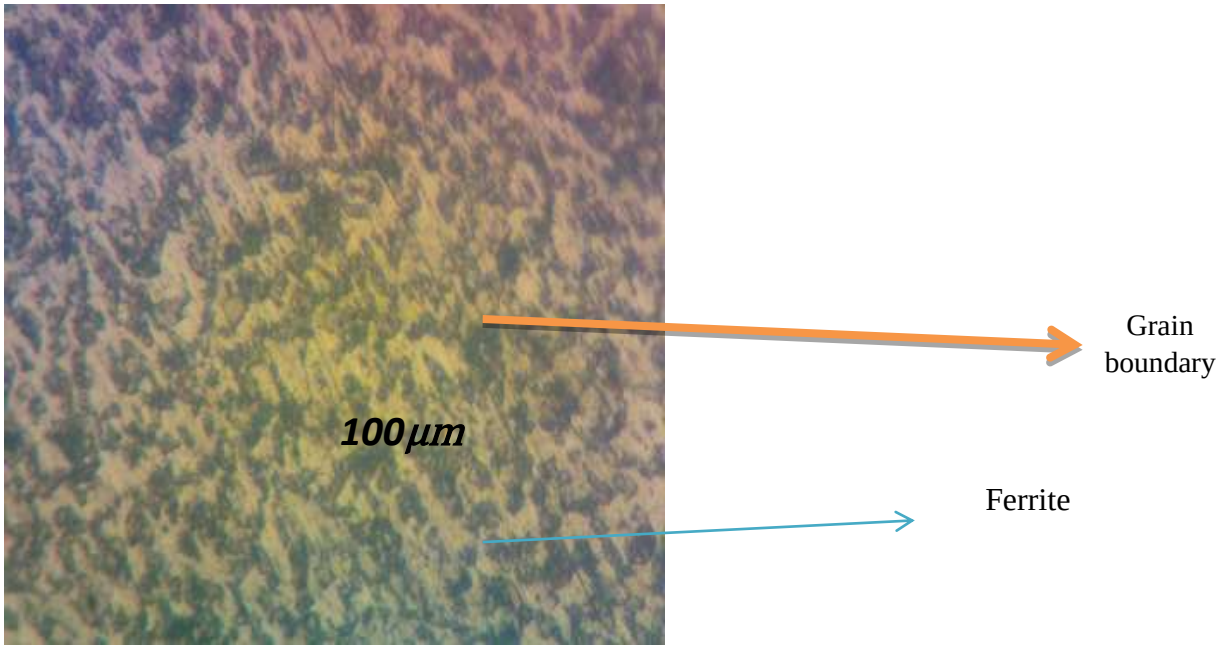

Plate 4.3d Microstructure of Specimen held at 930^{0}C for 90 Minutes

Plate 4.3d displays the microstructure of a heat-treated (annealed) sample obtained at a temperature of 930°C and a holding time of 90 minutes. Ferrite is seen to be non-uniformly distributed in the microstructure. It could be observed also that the grains boundaries were invisible. Results from the point count shows that ferrite is 42% in the microstructure while cementite is 58%.

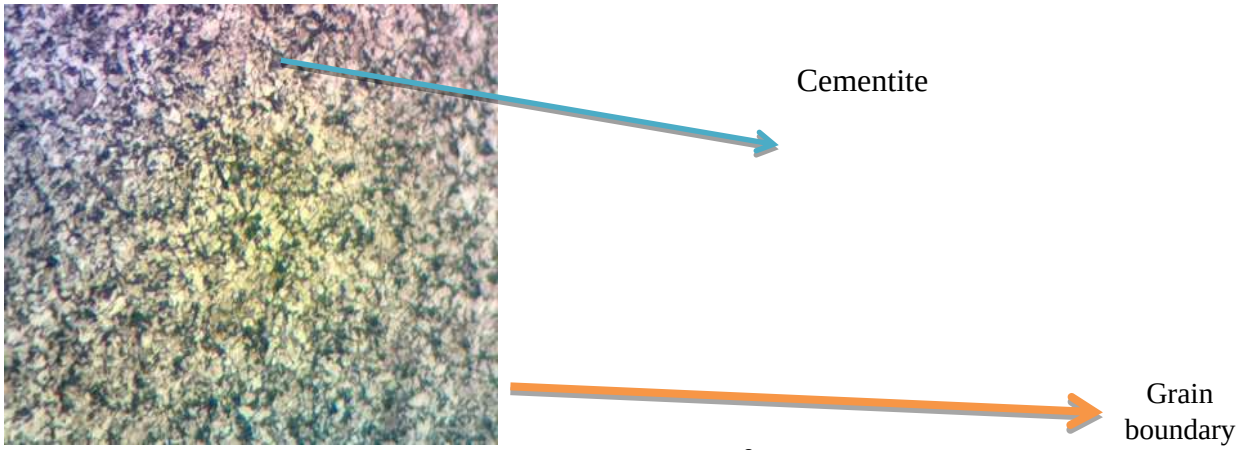

Plate 4.3e Microstructure of Specimen held at 960^{0}C for 90 Minutes

Plate 4.3e displays the microstructure of a heat-treated (annealed) sample obtained at a temperature of 960°C and a holding time of 90 minutes. Cementite is seen to be uniformly distributed and dominating in the microstructure while ferrite is seen to be uniformly distributed in the microstructure. It could be observed also that the grains boundaries were invisible. Results from the point count shows that ferrite is 49% in the microstructure while cementite is 51%.

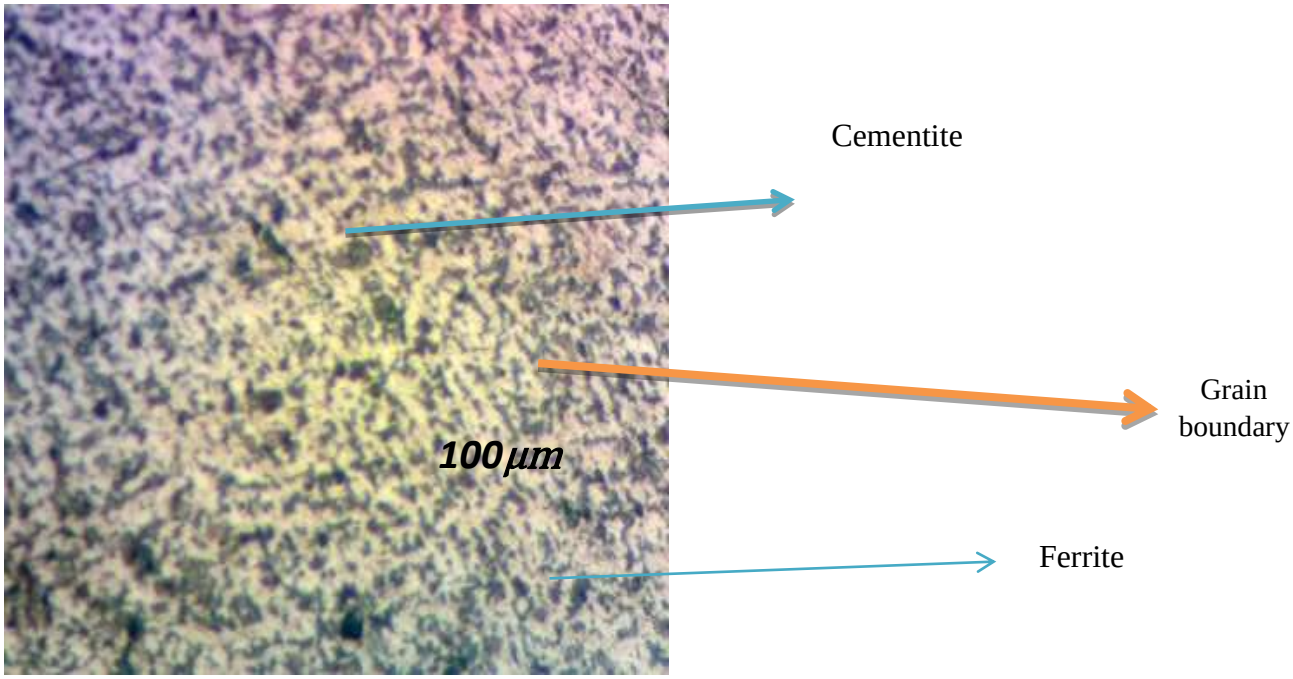

Plate 4.3f Microstructure of Specimen held at 990^{0}C for 90 Minutes

Plate 4.3f displays the microstructure of a heat-treated (annealed) sample obtained at a temperature of 990°C and a holding time of 90 minutes. Cementite is seen to be uniformly distributed and dominating in the microstructure while ferrite is seen to be uniformly distributed in the microstructure. It could be observed also that the grains boundaries were invisible. Results from the point count shows that ferrite is 46% in the microstructure while cementite is 54%.

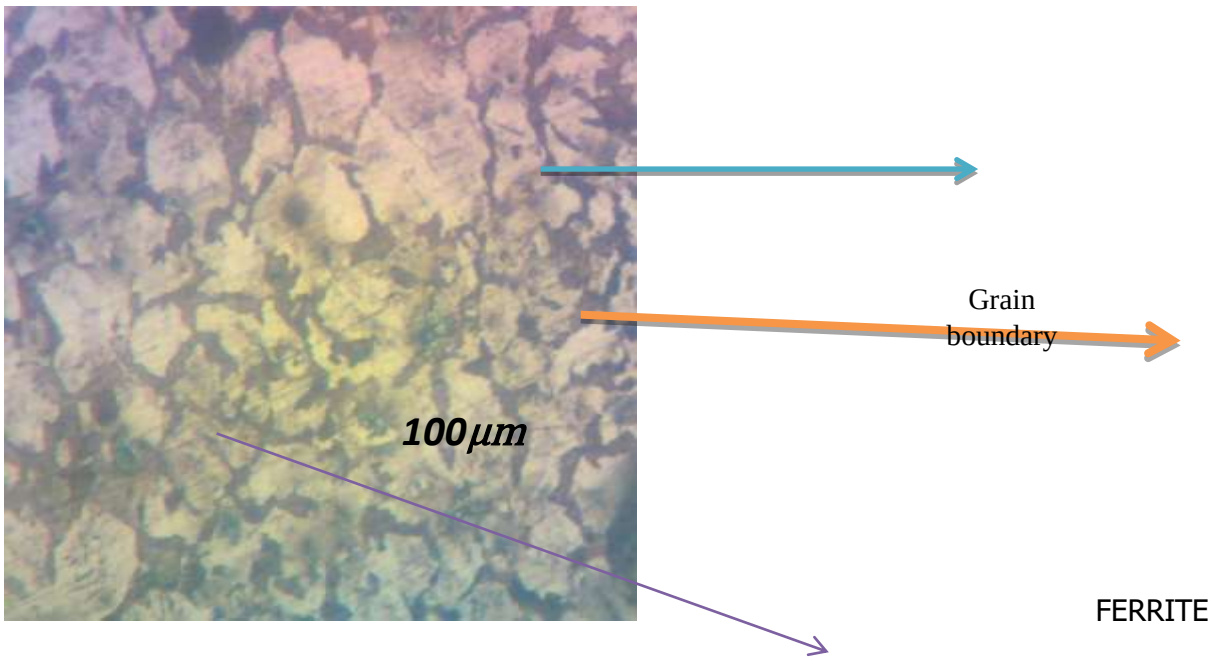

Plate 4.4a Microstructure of Specimen held at 840^{0}C for 120 Minutes

Plate 4.4a displays the microstructure of a heat-treated (annealed) sample collected at an annealing temperature of 840^{o}C and a holding time of 120 minutes. It could be observed that as the temperature increases, ferrite significantly increased and dominated in the microstructure. The

micrograph shows the grain boundaries as being visible. From the point count calculation the percentage the percentage of ferrite to cementite ratio is 54:46.

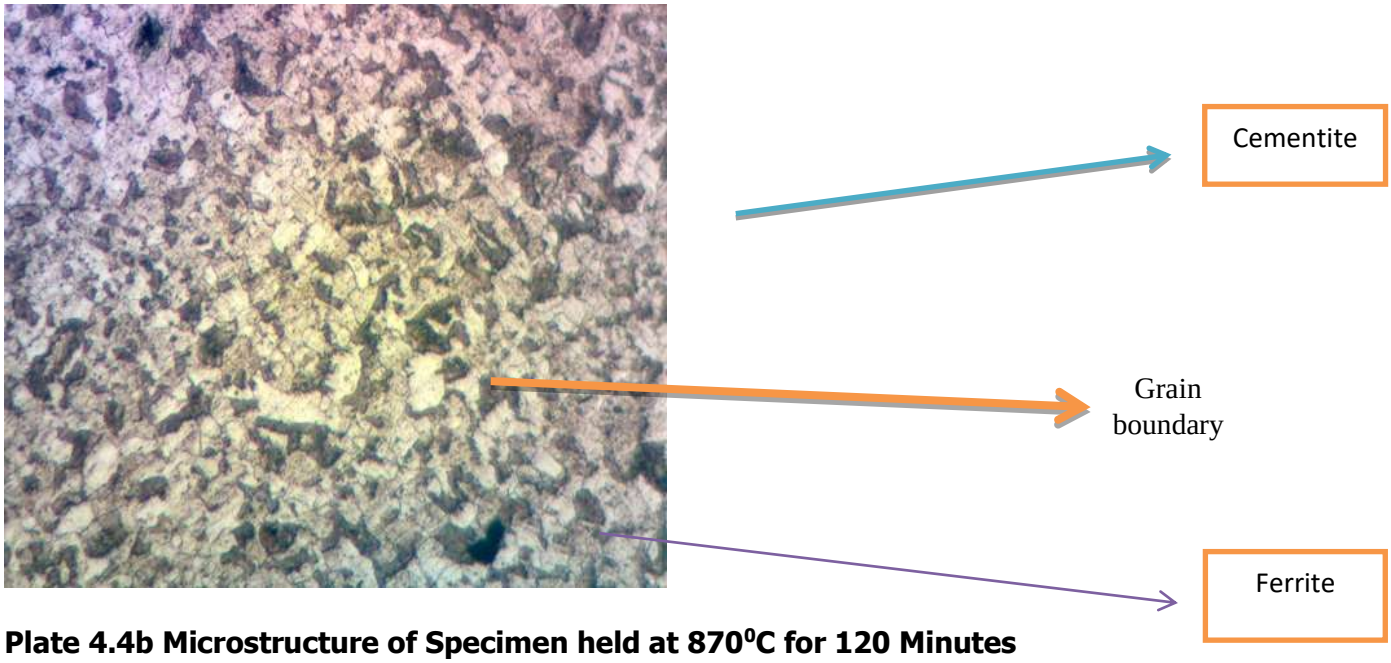

Plate 4.4b Microstructure of Specimen held at 870^{0}C for 120 Minutes

Plate 4.4b depicts the microstructure of a heat-treated (annealed) sample obtained at an annealing temperature of 870°C and a holding time of 120 minutes. At this temperature, cementite increased in percentage as the grains became coarser, resulting in less grains and grain boundaries; ferrite often dispersed in a non-uniform manner in the microstructure. The grain boundaries are not apparent in the micrograph. According to the point count, ferrite makes up 43% of the microstructure, while cementite makes up 57%.

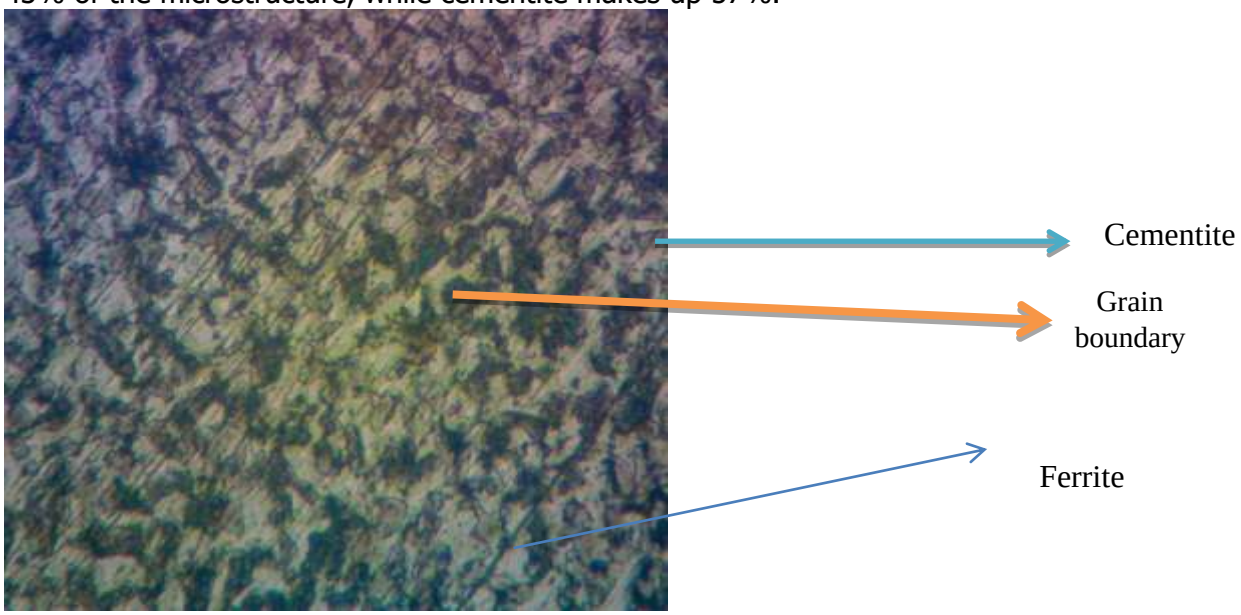

Plate 4.4c **Microstructure of Specimen held at 900^{0}C for 120 Minutes**

The microstructure of the heat-treated (annealed) sample obtained at 900^{o}C annealing temperature and 120 minutes holding time is shown in Plate 4.4c. The microstructure of cementite

increased as the temperature increased, while the grains were coarser than at 870^{0}C, resulting in less grains and grain boundaries; ferrite also distributed evenly in the microstructure. The grain boundaries are invisible in the micrograph. The proportion of ferrite to cementite ratio is 51:49, according to the point count estimate. The microstructure of the heat-treated (annealed) sample obtained at 900^{o}C annealing temperature and 120 minutes holding time is shown in Plate 4.4c.

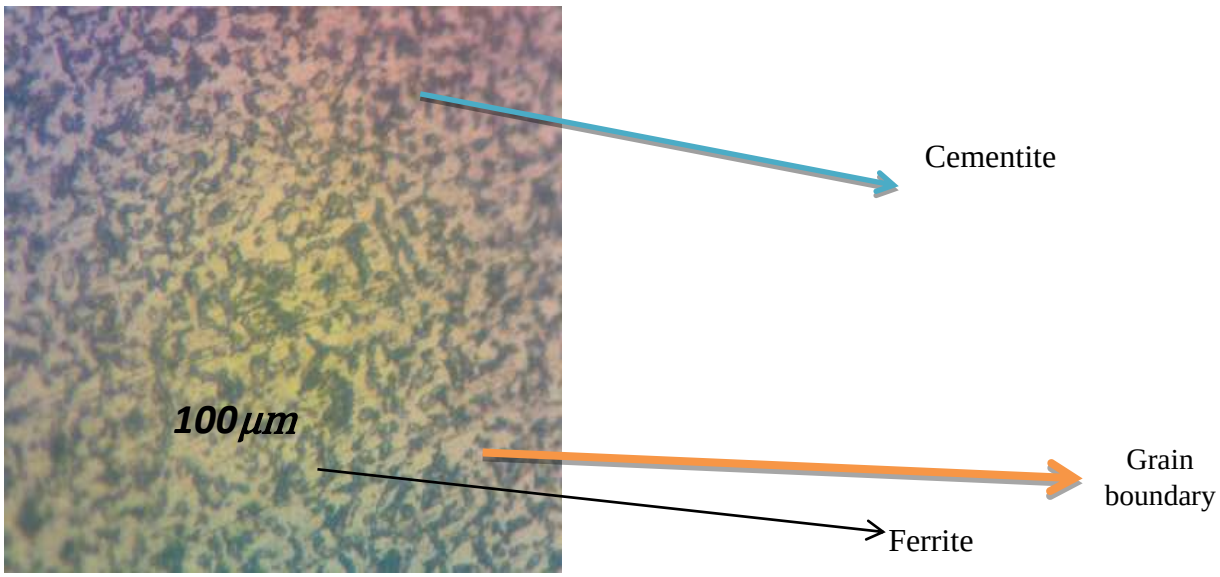

Plate 4.4d **Microstructure of Specimen held at 930^{0}C for 120 Minutes**

Plate 4.4d captures the microstructure of a heat-treated (annealed) sample obtained at an annealing temperature of 930^{o}C and a holding time of 120 minutes. The microstructure of cementite increased as the temperature increased, while the grains were less coarse than those of 900^{0}C, resulting in more grains and grain boundaries; ferrite was also evenly distributed in the microstructure, with cementite prevailing. The grain boundaries are invisible in the micrograph. The proportion of ferrite to cementite ratio is 47:53, according to the point count estimate.

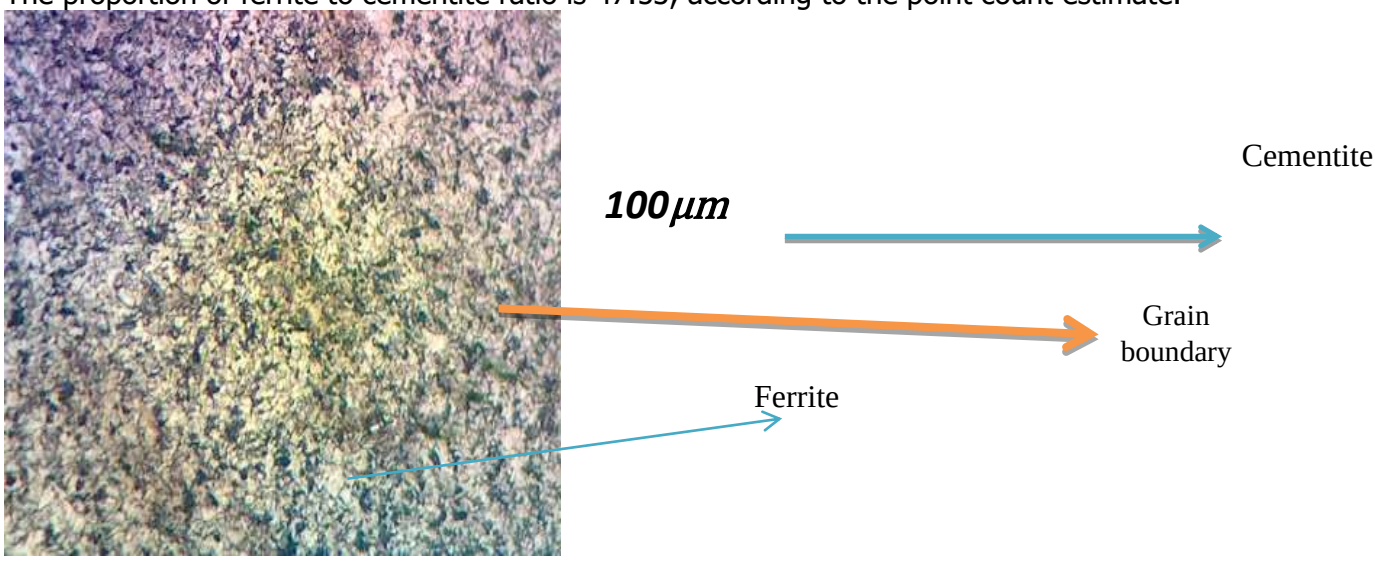

Plate 4.4e Microstructure of Specimen held at 960^{0}C for 120 Minutes

Plate 4.4e displays the microstructure of a heat-treated (annealed) sample obtained at an annealing temperature of 960^{o}C and a holding time of 120 minutes. It was noticed that as the

temperature rose, cementite increased and dominated in the microstructure, while the grains were changed more than at 930^{0}C, resulting in more grains and grain boundaries; ferrite was observed to be very few in the microstructure. The grain boundaries are invisible in the micrograph. According to the point count estimate, the ferrite to cementite ratio is 43:57.

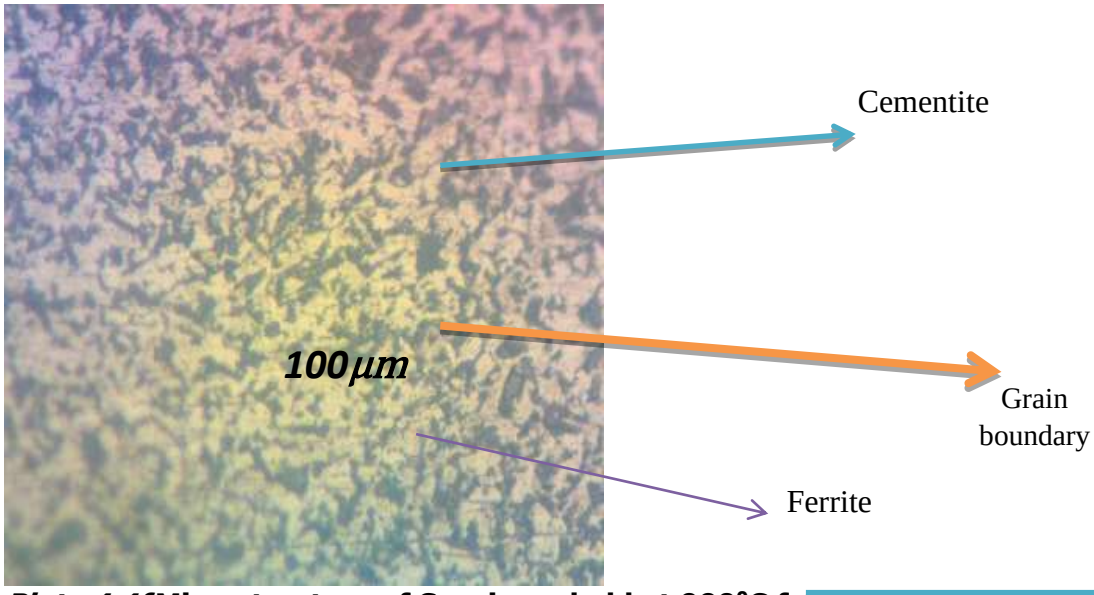

Plate 4.4f **Microstructure of Specimen held at 990^{0}C for 120 Minutes**

Plate 4.4f depicts the microstructure of a heat-treated (annealed) sample obtained at an annealing temperature of 990^{o}C and a holding time of 120 minutes. As the temperature increased, cementite significantly increased and dominated in the microstructure, while the grains were seen to be changed, resulting in more grains and grain boundaries; ferrite was seen to be non- uniformly distributed in the microstructure. The grain boundaries are invisible in the micrograph. According to point count calculations, the ferrite to cementite ratio is 42: 58.

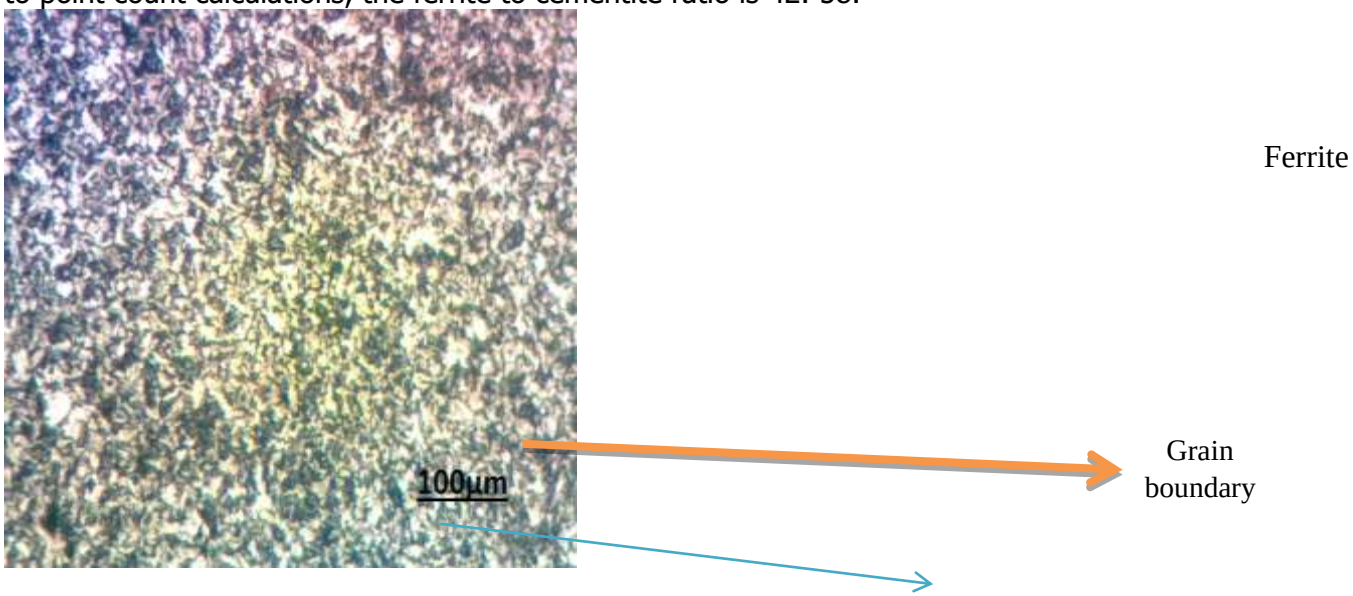

Plate 4.4g As Received

Plate 4.4g depicts the microstructure of the as-received sample; cementite increased and dominated the microstructure, while the grains were less coarse, resulting in more grains and grain boundaries; ferrite was found to be distributed unevenly in the microstructure. In the

micrograph, the grain boundaries are not clear. The calculation of point counts shows that the ferrite to cementite ratio in the microstructure is equally distributed, suggesting a 50:50 ratio.

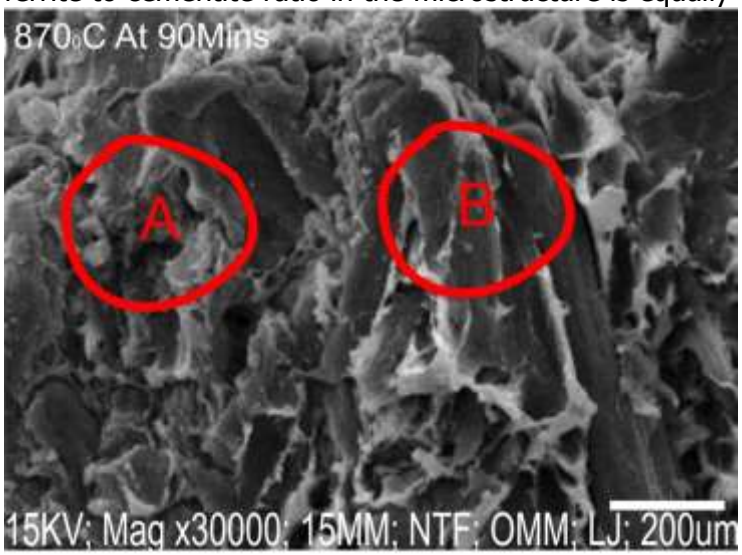

Plate 4.7 SEM of 870^{o}C at 90 minutes

Plate 4.7: Plate 4.6.reveals the SEM images of the fractured surfaces of broken fatigue samples at 870^{O} C annealing temperature and 90 minutes soaking time. The fractured surfaces shows essentially some fibrous characterized by some cleavage facets can be seen on the surface.

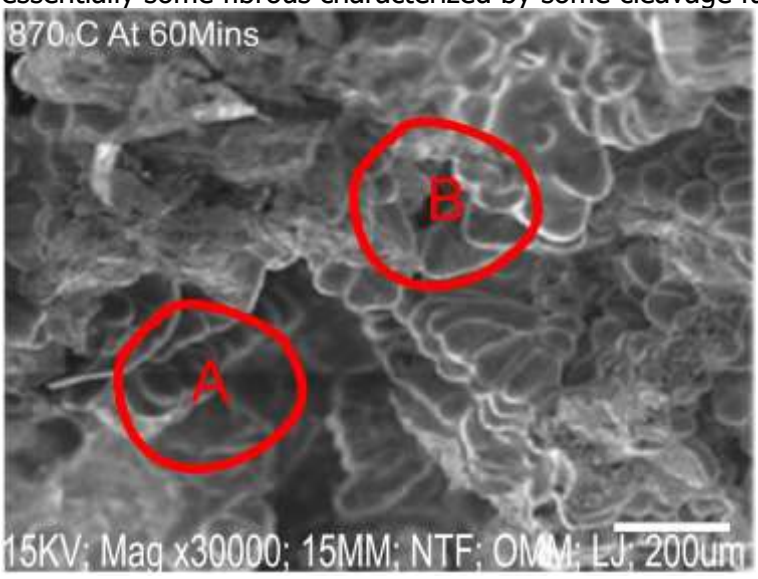

Plate 4.8 SEM of 870^{o}C at 60 minutes

Plate 4.8 reveals the SEM images of the fractured surfaces of broken fatigue samples at 870^{O}C annealing temperature and 60 minutes soaking time the fractured surface at 870^{O}C for 60 minutes showed annealed sample that exhibits a predominantly ductile surface which is different from honey comb morphology in 840^{O}C but some micro voids can be seen.

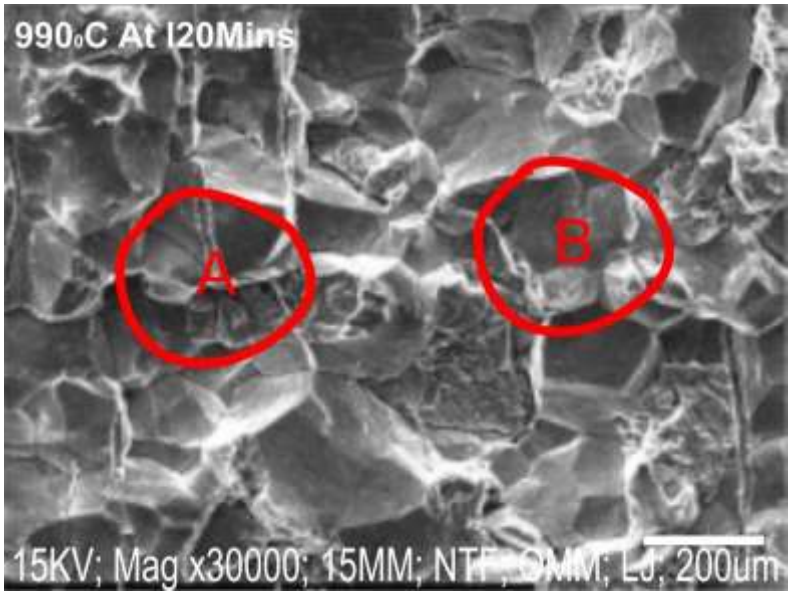

Plate 4.9 SEM of 990°C at 120 minutes

Plate 4.9 reveals the SEM images of the fractured surfaces of broken fatigue samples at 990^{O} C annealing temperature and 120 minutes soaking time. It shows that there were some micro dimples with ductile character region. There is detail of intergranular faceted fracture in (b) but in (c) we have more fine – faceted cleavage and detail of a deep crack probably due to the high temperature and longer time in the furnace. It was also observed that in 990°C for 120 minutes (b). There is also a crack propagation area with fatigue striations at 990°C for 120 minutes

Plate 4.10 shows the fractured fatigue sample of the as-received, this sample was not subjected to any heat treatment procedures. The phase still retains the ferrite and pearlite phases, however since fatigue work was done on the sample and they were all fractured .There were wide distributions of micro voids resembling microstructure and crack facets at the fractured tips making it brittle compared with the ones that were subjected to heat treatment mechanism. They are not faceted like the annealed ones, and do not have sharp edges and corners. They are less ductile compared with the ones that were annealed.

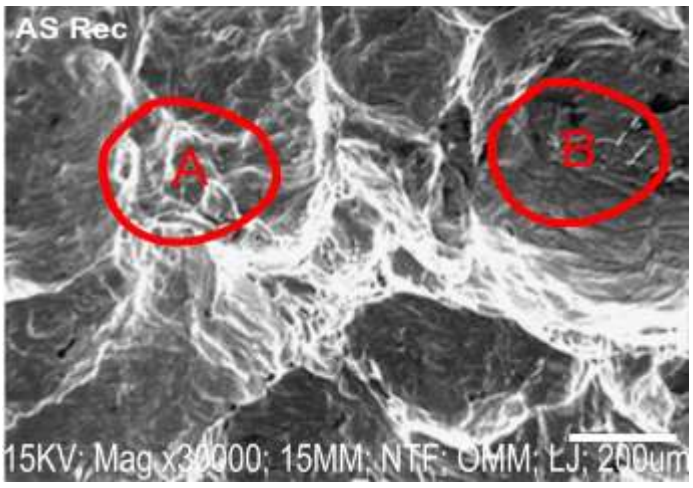

Plate 4. 10 SEM of As-Received

Plates 4.1a-4.1f display the microstructure of annealed steel as shown by an optical microscope after 30 minutes of soaking time at a magnification of X640 for the following: (4.1a) microstructure evolution at 840^{o}C, (4.1b) microstructure evolution at 870^{o}C, (4.1c) microstructure evolution at 900^{o}C, (4.1d) microstructure evolution at 930^{o}C, (4.1e) microstructure evolution at 960^{o}C, and (4.1f) microstructure evolution at 990^{o}C The microstructure evolution of the annealed sample is depicted in Plates 4.1a-4.1f, while Table 4.1 provides a quantitative estimate of the formed microstructures. Table 4.1 reveals that at 840^{o}C, the percent Ferrite was 44, while at 870^{o}C, the percent cementite was 56. (4.1b). at 900^{o}C, the percent ferrite appears to have decreased to 42 percent, while the percent cementite appears to have increased to 58 percent. 4.1c) both ferrite and cementite had the same proportion of 50. In Plate 4.1d, ferrite is seen to decrease in percentage and has 40% appearance versus cementite, which has 60% at 960^{o}C. According to the point count method, the percent ferrite and cementite in (4.1e) were equal. At 990^{o}C (4.1f), the percentage of ferrite was seen to have decreased to 47 percent in appearance, while cementite was 53 percent in the microstructure; this agrees with Rajan et al (2012)'s work, which states that cementite is present in steels that must have been cooled slowly because cementite formation is diffusion regulated. Plate 4.2a-Plate 4.2f shows the microstructure of annealed steel by optical microscope at 60 minutes soaking time at magnification of X640 for the following: (4.2a) microstructure evolution at 840^{o}C, (4.2b) microstructure evolution at 870^{o}C. (4.2c); microstructure evolution at 900^{o}C, (4.2d) microstructure evolution at 930^{o}C, (4.2e) microstructure evolution at 960^{o}C and (4.2f) microstructure evolution at 990^{o}C. In The microstructure evolution of the annealed sample is depicted in Plate.4.2a-4.2f, and the quantitative estimate of the formed microstructures is presented in Table 4.2. Table 4.2 shows that at 840^{o}C, the percent Ferrite was 40%, while at 870^{o}C, the percent Cementite was 60%. (4.2b). at 900^{o}C, the percent ferrite appears to have increased significantly to 80 percent, while the percent cementite appears to have decreased to 20%. At (4.2c), ferrite is seen to have decreased by 15%, taking it to 65 percent in the microstructure, while cementite was 35%. Plate 4.2d shows that as the temperature is raised to 930^{o}C, the percentage of ferrite decreases to 30% and the percentage of cementite increases to 70%. At 960^{o}C (4.2e), the percent ferrite has increased to 35 percent, compared to 65 percent for using the cementite point count process. At 990^{o}C (4.2f), the percentage of ferrite was seen to have increased further to 48 percent in appearance while cementite was 52 percent in the microstructure; this agrees with Rajan et al (2012) who attests to the fact that cementite is present in every steel which must have been cooled slowly because cementite formation is diffusion controlled.

Plates 4.3a-4.3f display the microstructure of annealed steel under an optical microscope after 60 minutes of soaking at a magnification of X640 for the following: (4.3a) microstructure evolution at 840^{o}C, (4.3b) microstructure evolution at 870^{o}C (4.3c) Microstructure evolution at 900^{o}C (4.3d) microstructure evolution at 930^{o}C, (4.3e) microstructure evolution at 960^{o}C, and (4.3f) microstructure evolution at 990^{o}C, respectively. The microstructure evolution of the annealed sample is depicted in Plate.4.3a-4.3f, and the quantitative estimate of the formed microstructures is provided in Table 4.3. Table 4.3 shows that at 840^{o}C, the percent Ferrite was 44 percent, while the percent Cementite was 56 percent. At 870^{o}C (4.3b), the percent ferrite has increased and both tend to have the same percentage of 50%. At 900^{o}C (4.3c), ferrite is seen to have

decreased to 48 percent in the microstructure, while cementite is 52 percent. Plate 4.3d indicates that as the temperature increased to 930^{o}C, the percentage of ferrite decreased to 42 percent and the percentage of cementite increased to 58 percent. At 960^{o}C (4.3e), the percent ferrite has increased to 49 percent, compared to 51 percent for cementite using the point count process. At 990^{o}C (4.3f), the percentage of ferrite was seen to have decreased to 46 percent in appearance while cementite was 54 percent in the microstructure; this agrees with Rajan et al (2012) who attests to the fact that cementite is present in any steel which must have been cooled slowly because cementite formation is diffusion regulated.

Plates 4.4a-4.4g display the microstructure of annealed steel under an optical microscope after 120 minutes of soaking time at a magnification of x640 for the following: (4.4a) microstructure evolution at 840^{o}C, (4.4b) microstructure evolution at 870^{o}C, (4.4c) microstructure evolution at 900^{o}C, (4.4d) microstructure evolution at 930^{o}C, (4.4e) microstructure evolution at 960^{o}C, and (4.4f) microstructure evolution at 990^{o}C The microstructure evolution of the annealed sample is depicted in Plates.4.4a-4.4f, while Table 4.4 provides a quantitative estimate of the formed microstructures. Table 4.4 reveals that at 840^{o}C, the percent Ferrite was 43 percent, while at 870^{o}C, the percent Cementite was 57 percent. (4.4b), the percent ferrite appears to have increased significantly to 54 percent, while the percent cementite appears to have decreased to 46 percent at 900^{o}C. At (4.4c), ferrite was reduced to 51 percent of the microstructure, while cementite was 49 percent. Plate 4.4d indicates that as the temperature rises to 930^{o}C, the percentage of ferrite decreases to 47 percent and the percentage of cementite increases to 53 percent. At 960^{o}C temperature according to the point count process, the percent ferrite has decreased further to 43 percent at (4.4e) compared to 57 percent for cementite. After using the point count method at 990^{o}C (4.4f), the percentage of ferrite was found to be 42 percent in appearance and 58 percent cementite in the microstructure. Plate 4.4g shows that the as-received has an equal percentage of ferrite and cementite, which is 50%; according to Rajput, (2004), annealed steel has fine grain size, allowing for more grain boundaries that serve as a hindrance to dislocation. When this is achieved, the plastic deformation stage is difficult to initiate since its function is dependent on dislocation movement, which increases dislocation density. The increase in dislocation density makes travel along the planes extremely difficult, resulting in increased intensity (Rajput, 2004). Rajan et al (2012), also attested to the fact that cementite is present in any steel that must have been cooled slowly because cementite formation is diffusion regulated.

4.15.4 Effect of Annealing Temperatures on Impact Toughness and Hardness

A close analysis of Figures 4.3a-4.3d shows that the yield strength, tensile strength, and impact strength of the steel increased in value with increasing annealing temperature. On the other hand, the value of hardness decreased over time. Mechanical properties of steels are measurably influenced by grain size; at room temperature, for instance, effects, yield strength, fatigue, tensile, and so on all increase as grain size decreases (Dieter et al, 1967). According to the findings, annealing substantially increased the fatigue strength of the steel. Zhoo et al., 2018; Seeteja et al, 2017, Fadara et al, 2011, Nurudeen et al, 2012; Jia et al., Al-Qaabah. et al, 2003; Yu, et al, 2005 discovered that annealing relieves internal tension and improves ductility. One can also infer that annealing changed the

grain size of the steel and improved the fatigue properties of the steel, as Rajan et al,2012 observed that fine grained steels have higher fatigue strength than coarse grain steels because the finer the grain, the higher the yield strength and enhanced fatigue strength.

CONCLUSIONS

This study investigated the influence of annealing temperatures and soaking times on the fatigue characteristics of 0.17 percent C HSLA steel. The steel was annealed six times at different temperatures and four different soaking times. To better highlight the effect of annealing on the steel's fatigue characteristics. The following findings can be reached from the investigations conducted in this study.

The optimal heat treatment parameters (temperature and holding time) for 0.17 percent C annealing HSLA Steel were 990°C. and 110(using design expert) minutes soaking time respectivelWhen compared to the As-received sample that had not been annealed, the morphological microstructures revealed a mixture of ferrite and cementite. The impact and hardness properties of the steel, as well as the Fatigue property, were discovered to be affected by morphological microstructures. It was discovered that when the annealing temperature increases, the impact increased while the hardness decreased.

The SEM fractograph exhibits a wide distribution of micro voids resembling microstructure and crack facets at the broken tips. Annealing heat treatment was found to have influence on the fatigue properties of the steel under investigation. The annealed samples were found to have more number of cycles to failure when subjected to cyclic loading when compared to the as-received sample. The annealed samples were found to have between 2900- 3800 cycles when compared to the as- received with 900 number of cycles before failure. Using the Basquin parameter, the results show that fatigue life at a given stress amplitude is dependent on the fatigue strength coefficient, σ_a and the fatigue strength exponent, b, with b being the most significant factor. The magnitude of b decreased as the annealing temperature was increased.

ACKNOWLEDGEMENT

The authors, Emordi Ngozi Grace (Principal Researcher) and Ofili Nkechi Joy (Co-Researcher) gratefully acknowledge the financial support granted by the Tertiary Education Trust Fund (TETFund), Nigeria through the Institution Based Research (IBR) Interventions for the research.

REFERENCES

Abbaschian, ReedHill,.(2009). Physical Metallurgy Principles. 4th Edition

Abdel-Raouf, H., Topper, T. H. Topper, Carden, A. E., McEvily A. J. and Wells C. H. (1972). ASTM Special Technical Publication 520

Abdoos, H., Khorsand, H., Shahani, A. R., (2009)."Fatigue behavior of diffusion bonded powder metallurgy steel with heterogeneous microstructure", Materials & Design, 2009

Abou-Jahja, H. J., (1997). The Effect Of Heating Temperature And Distribution of Martensite on MECHANICAL Properties of a Dual Phase Steel.(Arabic and English): Proceedings of The Second Jordanian International Conference On Mechanical Engineering Amman, Jordan.2i, 853-865,Pub.Org.

Agbokwor,S. E., Neife. S. I., (2019). Investigation of the Effects of Soaking Time on the Properties of Stainless Steel. *American Journal of Mech anical and Materials Engineering*. Vol. 3, No. 3, 2019, pp. 47-52. doi: 10.11648/j.ajmme.20190303.11

Aliya, D. and Lampman, S., Physical Metallurgy Concepts in Interpretation of Microstructures, *Metallography and Microstructures,* Vol 9, *ASM Handbook*, ASM International, 2004, p. 44–70

Al-Qawabah, S. M. A., Alshabatat, and Al-Qawabeha, U. F., (2012). "Effect of Annealing Temperature on the Microstructure, Microhardness, Mechanical Behavior and Impact Toughness of Low Carbon Steel Grade 45" International Journal of Engineering Research and Applications (IJERA) ISSN: 2248-9622 www.ijera.com Vol. 2, Issue 3, May-Jun 2012, pp.1550-1553.

Arasu, T. P. Dhansekaram**,** R., Kumar, S. P., and Srinivasan, N. (2013). Effect of Hardness and Microstructure on En 353 Steel by Heat Treatment .International Journal of Engineering and Science, Vol. 2. pp 01-05.

Arunachalam, R., Annadurai, G.,(2011). J. Envoron Sci.Technol,4.64.

American Society of Materials (ASM) Handbook Committee (1991): Heat Treating. ASM International, Vol 4

ASM: Practical Guide to Image Analysis. ASM International, Philadelphia, 2000

American Society of Materials (ASM) international, materials park, Ohio USA www.asminternational.org, (2001):.Alloying: understanding the basics.

ASTM E10-12.(2012): Standard Test Method for Brinell Hardness of Metallic Materials, ASTM International, West Conshohocken, PA, www.astm.org

ASTM E23. 2008. Standard Test Method for Izod Bar Impact Testing of Metallic Materials, American Society of Testing and Materials

ASTM E1820 (2010). Standard Test Method for Measurment of Fatigue Toughness. Pub.
ASTM International USA.

Atadious, D., Bankole, W., Jimba, Oyejide, O. J. (2018). "Behavioral Corrosion Mechanism of Hot Worked Mild Carbon Steel Immersed in various Acidic Environments", International Journal of Advances in Scientific Research and Engineering.

Beata, B., Lukasz, Konat, Robert, J. (2017). "The Influence of Austenite Grain Size on the Mechanical Properties of Low-Alloy Steel with Boron", Metals

Bear, Ferdinad, P., and Russell Johnson ,jr. E., (1992). Mechanics of Materials 2nd Ed. New York: McGraw –Hill, Inc.

Beer &Johnson (2006). Mechanics of Materials 5th Edition McGraw Hill.

Benyounis, K. Y., (2008). "Multi-response optimization of CO"2 laser-welding process of Austenitic stainless steel", Optics and Laser Technology,200802.

Bhadeshia, H. K. D. H., and Honeycombe, (2006). Steel: Microstructure and Properties. 3rd edition, Pub. Butterworth-Heinemann.

Bidulská, J., Kvačkaj, T., Kočiško, R., Bidulský, R., Grande, M.A., Donič, T., Martikan, M., (2010). Influence of ECAP-Back Pressure on the Porosity Distribution. Acta Physica Polonica A, 117(5), 2010, 864–868. https://doi.org/10.12693/APhysPolA.117.864

Bimakr, Mandana, Russly, A., Farah, S. T., Noranizan, M. A., Md. Zaidul, I. S., and Ali, G., (2012). "Optimization of Ultrasound-Assisted Extraction of Crude Oil from Winter Melon (Benincasa hispida) Seed Using Response Surface Methodology and Evaluation of Its Antioxidant Activity, Total Phenolic Content and Fatty Acid Composition", Molecules.

Bin Li., (2008). "Supercritical carbon dioxide-induced melting temperature depression and crystallization of syndiotactic polypropylene", Polymer Engineering & Science, 08/2008

Blaoui, M. M, Mokhtar Z., Mustapha A., (2019). "Effect of medium carbon steel microstructure on tensile strength and fatigue crack growth", International Journal of Structural Integrity,

Boyer, H. E., (2015). Atlas Of Fatigue Curve ASM International.

Broome, J. B.,(1997). Development of a Robust Heat Treatment Process for Rockwell B-Scale Hardness Test Blocks. Masters Thesis, Massachuisetts institute of Technology.

Byun, J. S., (2003). "Non-metallic inclusion and intragranular nucleation of ferrite in Ti-killed CMn steel", Acta Materialia, 20030402

Callister, W. (2005). Materials Science and Engineering. An introduction 3rd ed. - New York John Wiley and Sons, Inc.

Chan, C. W., Lee, S., Smith, G. C., Donaghy, C., (2017). Fibre Laser Nitriding of Titanium and its Alloy in Open Atmosphere for Orthopaedic Implant Applications : Investigations on Surface Quality, Microstructure and Tribological Properties. Surface Coatings Technology, 309, 2017, 628–640. https://doi.org/10.1016/j.surfcoat.2016.12.036

Chan, C., Smith, G. C., Fibre laser joining of highly dissimilar materials: Commercially pure Ti and PET hybrid joint for medical device applications. Materials Design, 103, 2016, 278–292. https://doi.org/10.1016/j.matdes.2016.04.086

Carbon Equivalent Formulae in Relation to Hydrogen Cracking.https://www.twi-global.com/technical-knowledge/faqs/faq-what-is-the-difference-between-the-various-carbon-equivalent-formulae-used-in-relation-to-hydrogen-cracking.

Chawla, K. K., (1998). Mechanical Behavior of Materials, 4th ed., Prentic-Hall Inc., 1998.

Cruz, M. G. H, Vieceli, A. A, (2008). Methodology for Replacement of Conventional Steel by Micro Alloyed Steel in Bus Tubular Structures Mater.W29 pp 539-545.

Dang, A. T., Vo, T. T. and Le, V. P., (2014). Analyzing 2D structure images of piezoelectric ceramics using ImageJ. Int. J. Materials Chem., 4: 88-91. DOI:10,5923/J.ijmc.20140404.02.

Daniel, H., Herring (2005). Heat Treat Doctor 630-834-3017 .www.industrialheating.com Morden Steel and their Properties Handbook 268, Bethlehem Steel.Co 1949

Dearden, J., and O'Neill, H., A Guide to the Selection and Welding of Low Alloy Structural Steel" Transactions of the Institute of Welding. Vol 3,194; pp203-214.

Diógenes, A. N., C. P. Fernandes and E. A. Hoff. (2005). Grain size measurement by imagej analysis: An application in the ceramic and in the metallic industries. Proceedings of the 18th International Congress of Mechanical Engineering, Nov. 6-11, OuroPreto.

Dossett, J. L., Boyer, H. E. *Allied Pub. Priv. Ltd, India* (2006).

Dzupon, M., Parilak, L., Kollarova, M., Sinaiova, I., (2006). Dual Phase Ferrite Martensitic Steel Micro Alloyed With V-Nb", *Metalurgija*, v. 46, n. 1, pp. 15-20.

Edoziuno, F. O., Odoni, B. U., AlO, F. I., Nwaeju C. C., (2020). Dry Sliding Wear And Surface Morphological Examination Of An Aluminium Matrix Composite Reinforced With Palm Kernel Shell, Acta Metallurgica Slovaca 2020, VOL. 26, NO. 2, 54-62 54 DOI: 10.36547/ams.26.2.537.

Fadare, D. ADieter, G. E., (1988). Mechanical Metallurgy, Pub. McGraw Hill, Singapore3rd Ed. Mc-Grew Hill Pp 346-369.

Fadara, T. G. and Akanbi O.Y., (2011). Effect of Heat Treatment on Mechanical Properties and Microstructre of NST 37-2 Steel. Journal of Materials and Materials Characterization and Engineering , Vol 10, No.3, pp299-308.

Fatigue of Engineering Materials and Structures (1979). Vol 2,pp107-119. Perganon Press. Printed in Great Britain.

Fayomi, O. S. I., Joshua, T. O., Olatuja, F. H. Agboola. O., (2019). "Effect of annealing on the mechanical characteristics of steel welded joint", Procedia Manufacturing.

"Fracture of Engineering Materials and Structures",(1991). Springer Science and Business
Media LLC.

Frank Goodwin, (2005). "Metals", Springer Handbook of Condensed Matter and Materials Data.

Fukaura, K. Yokoyama, Y. Yokoi, D., Tsujii, N. and Ono, K., (2004). " Fatigue of cold-work tool steels: effect of heat treatment and carbide morphology on fatigue crack formation, life, and fracture surface observations", Metallurgical And Materials Transactions A, vol. 35A.

Forrest, Peter G.(1962): Fatigue of Metals Oxford New York, Pergamon Press.

Gayda, J. Kantzos, P. and Telesman, J., (2003). "The effect of heat treatment on the fatigue behavior of alloy 10", NASA/TM-2003-212473.

Gaurav, D. Sonawane, and Radhey M. Bachhav (2018): Analysis of Different Heat Treated Materials for Fatigue FailureAIP Conference Proceedings, 020020 (2018); https://doi.org/10.1063/1.5058257 Published Online: 28 September 2018.

Gladshtein, L. I., Larionova, N. P., Belyaev, B. F., (2012). "Effect of ferrite-pearlite microstructure on structural steel properties", Metallurgist.

Goriewa-duba, K., Duba, A., Wachowska, U., Wiwart, M., (2018). An Evaluation of the Variation in the Morphometric Parameters of Grain of Six Triticum Species with the Use of Digital Image Analysis. Agronomy, 8, 2018, 296. https://doi.org/10.3390/agronomy8120296

Guiyun, L. (1989). Improvement of fatigue life time of steel implanted with N after heat treatment. Vacuum, vol. 93, no.(2-4).

Hadidi-Moud, S. A. Mirzaee-Sisan, A., Truman, C. E., Smith, D. J., (2004). "A local approach to cleavage fracture in ferritic steels following warm pre-stressing", Fatigue & Fracture of Engineering Materials & Structures.

Hall, E. O., (1970). Yield Point Phenomena in Metals and Alloys —Plenum Press New York.

Hertz, H., (1996). On the Contact Of Rigid Elastic Solids and Hardness, Miscellaneous

Papers, Macmillan, London, pp 163-183.

Honeycombe, R. W. K.and Bhadeshia, H. K. D. H., (2000). Steels Microstructure and Properties, 2nd ed., Butterworth-Heinemann Publishing Ltd. Oxford, U.K.

Hu, J., Wang, S., Zhoa, X., and Yu, B., (2010). Structure and Performance of Welding Structure 2003 and Performance of Welding Joint of Q235 Steel Welded by SHS Welding Mechanical Engineering in China, Vol 5, issue 2 pp 189-193.

Humphrey, F. J. and Hatherly, M. Recrystallization and Related Annealing Phenomena, 2_{nd} Ed, Elsecier. Ltd, Amsterdam.

Jia, D., Ramesh, K. T. and E, Ma. (2003). Effect of Monocrystalline and Ultrafine Grain Sizes on Constructive Behaviour and Shear Bands in Iron. ActaMaterialia, Vol. 51, No.12,pp. 3495-3509. Doi:10.1016/51359-6454(03)00169-1

John, O. Olawale, Simeon A. Ibitoye. "Failure analysis of a crusher jaw", Elsevier BV, 2018

Joseph, O. O., Joseph, O. O., Leranoi, R. O., Ojidin O. S., (2014). Effect of Heat Treatment on Micrstructure and Mechanical Properties of SAE 1025 Steel: Analysis by One Way ANOVA

Joshua Pelleg, (2013). "Mechanical Properties of Materials", Springer Science and Business Media LLC.

Kadkhodapour, J., Butz, A., Rad, S. Z. (2011). Mechanisms of void formation during tensile testing in a commercial, dual-phase steel", *ActaMaterialia*, v. 59, n. 7, pp. 2575-2588.

Karanjule, D. B., Bhamare, S. S., Rao, T. H., (2016). "Variation of elastic modulus during cold drawing of seamless tubes and it's influence on springback", 2016 IEEE International Conference on Industrial Engineering and Engineering Management (IEEM).

Katarina, B. and R. Gejza, (2009): Qualification of microstructural parameter, ferrite-martensitedualphase steel by ImageJ analysis. MEAL.

Kempester, M.H.A.,(1984) :Materials for Engineers, 3rd Edition Hoodder and Stronghton.

Khalifa, T. A. (1988). Effect of Inclusions on the Fatigue Limit of a Heat-Treated Carbon Steel, Materials Science and Engineering A, vol.102, pp.175-180.

Kim, W. J., Jeong, H. G. and Jeong, H, T., (2009). Achieving High Strength and Ductility on Magnesium Alloys using severe Plastic Deformation Combined with Low-Temperature Aging. SciptaMaterialia, Vol61, No. 11, pp1040-1043. Doi.10-1016/jscriptanat. 2009.08.020

Kipanyula, M. J., Sife, A. S. (2018). Global Trends in Application of Stereology as a Quantitative Tool in Biomed Research. Biomedical Research International. 2018, 2018, 1825697. https://doi.org/10.1155/2018/1825697 19

Krishnadev, M. R., Ghosh, R. and Galibois Effect of Low Temperature on the Fatigue properties of two High Strength Low Alloy Steel Pipeline Steels.

Kun, F., J. Stat. Mech. (2007) P02003; M. J. Alava, J. Stat. Mech. (2007) N04001.

Lee, J., Harry, B., Almond, D.P and Hammeh, F. (1997). Fabric Composite, Fatigue Life Determination, Composite, Part A Applieid Science and Manufacturing. Volume 28, Issue 1, pp. 5-13.

Les Pook, (2007). Metal Fatigue University College London. UK, Springer 2007.

Liang, J., Zhao, Z., Wu, H., Peng, C., Sun, B., Guo, B., Liang, J. and Tang, D. (2018): Mechanical Behavior of Two Ferrite–Martensite Dual-Phase Steels over a Broad Range

of Strain Rates. Metals **2018**, 8, 236.

Madariaga, I. Gutierrez, I., Bhadeshia, H. K. D. H., (2001). "Acicular ferrite morphologies in a medium-carbon microalloyed steel", Metallurgical and Materials Transactions A.

Mankins, W. L., (2004). Recovery, Recrystallization, and Grain-Growth Structures, *Metallography and Microstructures,* Vol 9, *ASM Handbook*, ASM International, 2004, p. 207–214

Manish, K. Madasu, L. V. Thang, Priyanka, C., Sree, P . "Peripheral kappa opioid receptor activation drives cold hypersensitivity in mice", Cold Spring Harbor.

Matilda, T. and Stefan, J., (2007). A Material Model for Simulation Volume Changes during Phase Transformations, Royal Institute of Technology KTH.

Mauricino, R. P., Arielton, T., William, H. T., Charles, L. I., Gregori, F., Andr, J., (2019). Fatigue Failure Analysis of HSLA Steel Sheets Holed by Conventional and Flow Drilling Process Revista Material ISSN 1517-7076 Article e-12374, V. 24 N.02.

Metal Fatigue Solid Mechanics and Applications, (2007). Vol 145. Springer, Dordreetit.
.
Miroslaw Szala, GrzegorzWiniarski, Lukasz Wojcikand Tomasz Bulzak, (2020). "Effect of Annealing Time and Temperature Parameters in the Microstructure, Hardness and Strain Hardening Coefficient of 42 CrMo4 Steel doi:10.20944/preprints 202004.0147 V1

Mubarak, A., Khan, Rashidul Alam, Md. Arifur Rahman, Farhana G., Noor, Ruhul A., Khan. (2009). "Physico-Mechanical and Degradation Properties of Urea-Modified Chitosan Film Photocured with 1-Vinyl-2 Pyrrolidone", Polymer-Plastics Technology and Engineering.

Nurudeen, A. R., Oluleke, O. O., (2012). Effect of Soaking Time on the Mechanical Properties of Annealed Cold-Drawn Low Carbon Steel *Materials Sciences and Applications*, 3, 513-518 doi:10.4236/msa.2012.38072 Published Online August 2012 (http://www.
SciRP.org/journal/msa) 513 Received February 21st, 2012; revised April 15th, 2012; accepted June 11th, 2012.

Obiukwu O., Udeani H., Ubani P. (2016). The Effect of Heat Treatment on the Mechanical Properties of SAE 1035 Steel *International Journal of Engineering and Technologies*

Offor, P. O., Ezekoye, V. O., and Ezekoye, B. A., (2010). Influence of Heat Treatment on The Mechanical Properties of 0.13 wt% Structural Steel. The Pacific Journal of Scientific and Industrial Research, 2(4): 611-615.

Oğurtani, T. (2014). Re what happens to the density of dislocation? Retrieved from https://www.researchgate.net/post/whathappens-to-the-density-of-dislocation/ 546c53dcd 3df3ebc1c8b4662/citation/download

Olawale, J. O. Ibitoye, S. A. "Influence of Casting Section Thickness on Fatigue Strength of Austempered Ductile Iron", Journal of Materials Engineering and Performance, 2017

Olson, E., (2011). Particle Shape Factors and Their Use in Image Analysis – Part 1: Theory. Journal of GXP Compliance, 15(3), 2011

Onyekpe, B.O.(2002). 'The Essentials of Metallurgy and materials in Engineering'. Ambik Press Benin City

Orkun, U. O., (2003). Effect of Temperature on Fatigue Properties of Din35NiCrMoV125 Sheet A Thesis Submitted to The Graduate School of Natural and Applied Sciences of the Middle East Technical University.

Pengpeng, Q., Mingcan, C., Kyounglim, K.,. Beomguk, P., Yonggyu, S., Eunkyung Khim, Min, J., and Jeehyeong,(2013). K. "Application of Box-Behnken design with response surface methodology for modeling and optimizingultrasonic oxidation of arsenite with H2O2", Central European Journal of Chemistry.

Philippidis, T. P., Vassilopou, A.P, (1999). Fatigue Of Composite Laminated Under Off-Axis Loading, International Journal of Fatigue, Volume 21, Issue 3, pp 253-262. Pook, L.
(2007): Metal Fatigue, University College London, Uk, Springer.

Pope, J. A., (1959): Metal Fatigue London, Chapman & Hall Ltd

Policena, M. R., Trindade, A., Fripp,, W.h., Isreal,C.I., Fronza,G. and Joao de Souza, A. (2019): Fatigue Failure Analysis of HSLA Steel Sheets Holed by Conventional and Flow Drilling Processes. Revisita Materia 24 .https.//doi.org/10.1590/s1517-707620190003.0784

Rajan, T. V., Sharma, C. P., Sharma, A. (2012). Heat Treatment Principles and Techniques 1st Ed, Practice- Hall, New Delhi.

Rajakumar, S., (2011). "Multi-Response Optimization of Friction-Stir-Welded AA1100 Aluminum Alloy Joints", Journal of Materials Engineering and Performance.

Rajput, R.K. (2004). "A Textbook of Material Science and Engineering", (3rd edition). S.K. Kataria &sons, Delhi, India.

Rashid, M. S., (1980). High Strength, Low Alloy Steel, Science, 208 (4146):862-869.

Raymon A., Higgins B., (1985). Properties of Engineering Materials Hodder and Stronghton.

Ricardo B., and FilippO, B. (2018). Mechanical Behavior of High-Strength, Low-Alloy Steels Metals (2018): 8, 610; doi:10.3390/met8080610 www.mdpi.com/journal/metals

Rojas, J., Hernandez C., Trujillo D.(2014). "Effect of the alkaline treatment conditions on the tableting performance of chitin obtained from shrimp heads", African Journal of Pharmacy and Pharmacology.

Roselita, F., Stelios ,K., Georgios ,S., Nikolaos, M. (2014). "The Effect of Heat and Surface Treatment on the Fatigue Behaviour of 56SiCr7 Spring Steel", Procedia Engineering.

Sajjia, M., Benyounis, K. Y., Olabi. A. G., (2012). "The simulation and optimization of heat treatment of cobalt ferrite nanoparticles prepared by the sol– gel technique", Powder Technology.

Sanjeev, K. Garg, Alakesh, M., Ajai Jain(2014). "An Investigation on Machinability of Al/10 % ZrO2(P)-Metal Matrix Composite by WEDM and Parametric Optimization Using Desirability Function Approach", Arabian Journal for Science and Engineering.

Satsh Kumar S.R., and Santha kumar, A.R. Design of Steel Structures, Indian Institute of Technology Madras.

Schneider, C. A., W.S. Rasband and K.W. Eliceiri, (2012). NIH image to imageJ: 25 years of image analysis. Nat. Methods, 9: 671-675 https:// doi: 10.1038/nmeth.2089.

Schindler, J. Jonosec, M.,Mistcaky, E.Ru,M., Zicka, L.A.,Cizek, Dobizdviski, Rusz,S. and Segurala,J., Allen,N.S.Edge,M.,Mahon,A.M.(1999) Prog.Coat. 37,23.

Senthil, S., Pradeep, S., Senthamaraikannnan, P., Sanjay, M. and Mohammad Jawaid, P. (2018). Characterization and Properties of Natural Fibrer Polymer Composites: A Comprehensive Review. Journal of Cleaner Production, 172,566-581. https://doi.org/10.1016/j.jcleprpo.2017.10.101

Sharma, A. M., (2016). Fatigue Properties of High Strength-Low Alloy Steel, Springer.com.

Singh V., for standard publisher's distributors, Delhi, 2008, pp.417.

Soh, B. D., Totsing, Anago, G. I., Fogue, M. (2010). International Journal of Engineering.
Vol. 125 pp 477-481.

Somer, M. Nacy, (2007). Effect of Heat Treatment on Fatigue Behavior of (A193-51T-B7) Alloy Steel Proceedings of the World Congress on Engineering 2007 Vol II WCE 2007, July 2 - 4, 2007, London, U.K.

Sreeteja, M.,Pranavadithya, S., Nitish, V. and GundaSowmya. (2017).Experimental Investigation on the Effect of Annealing on Fatigue Life of SAE 202 and 440C Steels. International Journal of Current Engineering and Technology.Vol.7, No. 3 p 857-861.

Stephens, R. I., Bradley, N. J., Horn, N. J. Gradman, J. J. Arkama, J. M. and Borgward (2005). C. S. 'Fatigue of High Strength Bolts Rolled before and after Heat Treatment with five different preloaded levels'.

Stoyka, V., Kovac, F. and Julius, B., (2009). Study of Secondary Recrystalization in Grain Oriented Steel Treated under Dynamic Heat Treatment Conditions, METABK,Vol48, No 2, pp 99-102.

Svenaneki, (2009). Effect of Cold Rolling and Annealing on Mechanical Properties of HSLA Steel. Achieves of Materials Science and Engineering, Vol.36, No.1pp41-47.

Tarkeshwar, S., Devjyoti, L., Ayush, K. (2017). "Effects of Various Parameters on Structural and Optical Properties of CBD-Grown ZnS Thin Films: A Review", Journal of Electronic Materials, 2017

Tewary, N. K., Ghosh, S. K., Chatterjee, S., (2015). Effect of Annealing on Microstructure and Mechanical Behaviour of Cold Rolled Low C, High Mn TWIP Steel. International Journal of Metallurgical Engineering 2015, 4(1): 12-23 DOI: 10.5923/j.ijmee. 20150401.03

To Shi Oka, Y., Heat Treatment Deformation of Steel Production (1985). Material Science Technology 1, 883-892.

Vander Voort, G. (2005)."Microstructure of Ferrous Alloys", Analytical Characterization of Aluminum Steel and Superalloys.

Vervynckts, S. Thibamx, P., Verbeken, K. (2012). Effect of Niobium on Microstructure and Mechanical Properties of Hot Rolled Micro alloyed Steels after Recrystallization-Controlled Rolling. Met Material int., 18: 37-46.

Wang, X.T., Siwecki,T.and Engberg,
G.(2003): Yield Point Phenomenal in Metals and Alloys(1970): E.O. Hall Plenum Press. New York.

Wang, K. F., Wang, S., Chandraseker, Yang, H. T. Y., (1997). Experimental and Computational Study of the Quenching of Carbon Steel Product's Material Science P 257-265.

William, D. Jr. (1994). Materials Science and Engineering, an Introduction to 3rd Ed-Callister, New York John Willey and sons Inc.

Xiaolei Xu, Zhiwei Yu. (2007). "An investigation on the failed blades in a locomotive turbine", Engineering Failure Analysis.

Xu, W., Westerbaan, D., Nayak, S. S., Chen, D. L., Goodwin, F., Zhou, Y., (2013). "Tensile
and fatigue properties of fiber laser welded high strength low alloy and DP980 dual-phase
steel joints", Materials & Design.

Ye D.Y., (1996). A new approach to the prediction of fatigue notch reduction factor Kf, International Journal of Fatigue, vol.18, , pp.105-109.

Yu, C. Y., Sun, P.L, Kao, P. W. and Chang, C. P., (2005). Mechanical Properties of Submicro-
Grained Aluminium" ScripaMaterialia, Vol 52, No. 5, pp. 359-363. Doi:10.1016Ij. Scriptamat.2004.10.035.

Zhang, Z.M., Zheng, H.I.,Hazard, J.: (2009) Mater 172: 1388.

Zhao, J., Jiang, Z. & Lee, C. Soo. (2013). Enhancing impact fracture toughness and tensile
properties of a microalloyed cast steel by hot forging and post-forging heat treatment processes. Materials and Design, 47 227-233.

Zhao J., Lee J.H., Kim Y.W., Jiang Z, Lee CS. Enhancing mechanical properties of a low-

Carbon micro alloyed cast steel by controlled heat treatment. Material .Sci. Eng A2013; 559:427-35.

Zhoa, Z, Wu, H., Peng, C., Sun, B., Guo, B., Liang, J. and Tang, D., (2017). Mechanical
Behavior of Two Materials. Proceedings of the 18th International Congress of Mechanical
Engineering, Ouro Preto, 6-11 November 2017.

Zhiwei Yu, Xiaolei Xu.(2006). "Failure analysis cases of components of automotive and locomotive engines", Elsevier BV.

Zhuang Li, Di Wu, Wei Lu, (2015). Effect of Holding Time on the Microstructure and Mechanical Properties of Dual- Phase Steel During Intercritical Annealing. Journal of Wuhan University of Technology- Mater.Sci.Ed., Volume 30, Number 1, page 156.

Zhuming Bi, Xiaoqin Wang. (2020). "Computer Aided Design and Manufacturing", Wiley, 2020

.